(12) INTERNATIONAL APPLICATION PUBLISHED UNDER THE PATENT COOPERATION TREATY (PCT)

(19) World Intellectual Property Organization
International Bureau

(43) International Publication Date
7 February 2013 (07.02.2013)

WIPO | PCT

(10) International Publication Number
WO 2013/019257 A1

(51) International Patent Classification:
B82Y 30/00 (2011.01) *B08B 17/06* (2006.01)
B05D 5/08 (2006.01)

(21) International Application Number:
PCT/US2011/061498

(22) International Filing Date:
18 November 2011 (18.11.2011)

(25) Filing Language: English

(26) Publication Language: English

(30) Priority Data:
61/514,794 3 August 2011 (03.08.2011) US

(71) Applicant *(for all designated States except US)*: **MASSACHUSETTS INSTITUTE OF TECHNOLOGY** [US/US]; 77 Massachusetts Avenue, Cambridge, MA 02139-4307 (US).

(72) Inventors; and

(75) Inventors/Applicants *(for US only)*: **DHIMAN, Rajeev** [CA/US]; 8 Island Hill Avenue, No. 213, Malden, MA 02148 (US). **BIRD, James, C.** [US/US]; 1010 Memorial Drive, Apt. 17P, Cambridge, MA 02139 (US). **KWON, Hyukmin** [KR/US]; 143 Albany Street, Apt. 235, Cambridge, MA 02139 (US). **VARANASI, Kripa, K.** [IN/US]; 31 Fletcher Avenue, Unit 5, Lexington, MA 02420 (US).

(74) Agents: **HAULBROOK, William, R.** et al.; Choate, Hall & Stewart LLP, Two International Place, Boston, MA 02110 (US).

(81) Designated States *(unless otherwise indicated, for every kind of national protection available)*: AE, AG, AL, AM, AO, AT, AU, AZ, BA, BB, BG, BH, BR, BW, BY, BZ, CA, CH, CL, CN, CO, CR, CU, CZ, DE, DK, DM, DO, DZ, EC, EE, EG, ES, FI, GB, GD, GE, GH, GM, GT, HN, HR, HU, ID, IL, IN, IS, JP, KE, KG, KM, KN, KP, KR, KZ, LA, LC, LK, LR, LS, LT, LU, LY, MA, MD, ME, MG, MK, MN, MW, MX, MY, MZ, NA, NG, NI, NO, NZ, OM, PE, PG, PH, PL, PT, QA, RO, RS, RU, RW, SC, SD, SE, SG, SK, SL, SM, ST, SV, SY, TH, TJ, TM, TN, TR, TT, TZ, UA, UG, US, UZ, VC, VN, ZA, ZM, ZW.

(84) Designated States *(unless otherwise indicated, for every kind of regional protection available)*: ARIPO (BW, GH, GM, KE, LR, LS, MW, MZ, NA, RW, SD, SL, SZ, TZ, UG, ZM, ZW), Eurasian (AM, AZ, BY, KG, KZ, MD, RU, TJ, TM), European (AL, AT, BE, BG, CH, CY, CZ, DE, DK, EE, ES, FI, FR, GB, GR, HR, HU, IE, IS, IT, LT, LU, LV, MC, MK, MT, NL, NO, PL, PT, RO, RS, SE, SI, SK, SM, TR), OAPI (BF, BJ, CF, CG, CI, CM, GA, GN, GQ, GW, ML, MR, NE, SN, TD, TG).

Published:

— *with international search report (Art. 21(3))*

WO 2013/019257 A1

(54) **Title**: ARTICLES FOR MANIPULATING IMPINGING LIQUIDS AND METHODS OF MANUFACTURING SAME

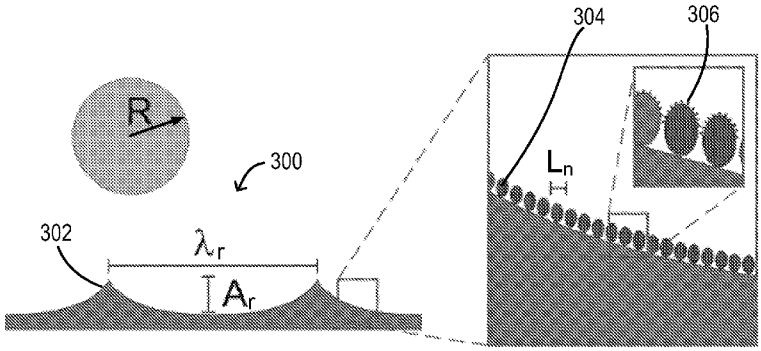

FIG. 3

(57) **Abstract**: This invention relates generally to an article that includes a non-wetting surface having a dynamic contact angle of at least about 90°. The surface is patterned with macro- scale features configured to induce controlled asymmetry in a liquid film produced by impingement of a droplet onto the surface, thereby reducing time of contact between the droplet and the surface.

ARTICLES FOR MANIPULATING IMPINGING LIQUIDS AND METHODS OF MANUFACTURING SAME

Cross-Reference to Related Application

[0001] This application claims priority to and the benefit of, and incorporates herein by reference in its entirety U.S. Provisional Patent Application No. 61/514,794, which was filed on August 3, 2011.

Field of the Invention

[0002] This invention relates generally to surfaces that manipulate impinging liquids. More particularly, in certain embodiments, the invention relates to macro-scale features on a surface that reduce the contact time between an impinging liquid and the surface.

Background of the Invention

[0003] Superhydrophobicity, a property of a surface when it resists contact with water, has been a topic of intense research during the last decade due to its potential in a wide variety of applications, such as self-cleaning, liquid-solid drag reduction, and water repellency. Water repellency of superhydrophobic surfaces is often studied by droplet impingement experiments in which millimetric drops of water are impacted onto these surfaces and photographed. With appropriate surface design, droplets can be made to bounce off completely. However, the time taken to bounce off – hereafter referred to as the contact time – is critically important as mass, momentum, and/or energetic interactions take place between the droplet and the surface during the time of contact. For example, the energy required to deice an airplane wing can be reduced if a water drop rebounds off the wing before it freezes.

[0004] Recent literature suggests there is a theoretical minimum contact time, t_c. *See* M. Reyssat, D. Richard, C. Clanet, and D. Quere, *Faraday Discuss.*, 2010, **146**, pp.19–33; and D. Quere, *Nature Letters*, 2002, **417**, pp. 811. Specifically, models that estimate the effects of contact line pinning on contact time have found that the contact time scales as

$$t_c \approx 2.2\left(\frac{\rho R^3}{\gamma}\right)^{1/2}\left(1+\frac{\phi}{4}\right) \quad (1)$$

where t_c is the contact time of a drop, of radius R, density ρ, and surface tension γ, bouncing on a superhydrophobic surface with pinning fraction ϕ. Even if one were able to completely eliminate this surface pinning such that $\phi = 0$, there would still be a minimum contact time limited by the drop hydrodynamics.

[0005] New articles, devices, and methods are needed to decrease the contact time between a droplet and a surface for improved liquid repellency. Contact times less than the theoretical minimum have heretofore been believed to be impossible.

Summary of the Invention

[0006] The articles, devices, and methods presented herein incorporate unique surface designs that can manipulate the morphology of an impinging droplet and lead to a significant reduction (e.g., more than 50% below the theoretical minimum prediction of Equation 1) in the time of contact between a droplet and its target surface. These designs are capable of improving the performance of a wide variety of products that are negatively affected by droplet impingement. Examples of such products include rainproof consumer products, steam turbine blades, wind turbine blades, aircraft wings, engine blades, gas turbine blades, atomizers, and condensers.

[0007] The articles, devices, and methods described herein offer several advantages over previous approaches in the field of water repellency using superhydrophobic surfaces. For example, the articles, devices, and methods lead to a major reduction (e.g., over 50%) in the contact time compared to the existing best reported contact time in the literature (i.e., the minimum contact time predicted by Equation 1, above). This surprising reduction in contact time is desirable not only to control diffusion of mass, momentum, or energy (depending upon the application), but also to prevent droplets from getting stuck on a surface due to impact from neighboring impinging droplets. In addition, the approach described herein is more practical and scalable as it relies on introducing macro-scale features that are easy to machine or fabricate with current tools. By contrast, previous approaches focus on the use of micron to sub-micron features that are difficult to fabricate and, at best, provide contact times that approach but do not fall below the minimum predicted by Equation 1. Contact times achieved using the articles, devices, and methods described herein are lower than those attainable with the lotus leaf (the best known superhydrophobic surface), which is limited by Equation 1.

[0008] The articles, devices, and methods described herein may be used in a wide variety of industries and applications where droplet repellency is desirable. For example, textile companies that manufacture rainproof fabrics, such as rainwear, umbrellas, automobile covers, etc., could significantly improve fabric waterproof performance. Likewise, energy companies that manufacture steam turbines could reduce moisture-induced efficiency losses caused by water droplets entrained in steam, which impinge on turbine blades and form films, thereby reducing power output. Condensers in power and desalination plants may utilize the devices and methods described herein to promote dropwise shedding condensation heat transfer. Further, in aircraft and wind turbine applications, a reduced contact time of supercooled water droplets impinging upon aircraft surfaces is desirable to prevent the droplets from freezing and thereby degrading aerodynamical performance. In atomizer applications, the ability of surfaces to break up droplets can be used to create new atomizers for applications in engines, agriculture, and pharmaceutical industries. In gas turbine compressors, the devices and methods described herein may be used to prevent oil-film formation and reduce fouling.

[0009] In one aspect, the invention relates to an article including a non-wetting surface having a dynamic contact angle of at least about 90°, said surface patterned with macro-scale features configured to induce controlled asymmetry in a liquid film produced by impingement of a droplet onto the surface, thereby reducing time of contact between the droplet and the surface. In certain embodiments, the non-wetting surface is superhydrophobic, superoleophobic, and/or supermetallophobic. In one embodiment, the surface includes a non-wetting material. The surface may be heated above its Leidenfrost temperature.

[0010] In certain embodiments, the surface includes non-wetting features, such as nanoscale pores. In certain embodiments, the macro-scale features include ridges having height A_r and spacing λ_r, with A_r/h greater than about 0.01 and λ_r/A_r greater than or equal to about 1, wherein h is lamella thickness upon droplet impingement onto the surface. In certain embodiments, A_r/h is from about 0.01 to about 100 and λ_r/A_r is greater than or equal to about 1. In one embodiment, A_r/h is from about 0.1 to about 10 and λ_r/A_r is greater than or equal to about 1.

[0011] In certain embodiments, the article is a wind turbine blade, the macro-scale features include ridges having height A_r and spacing λ_r, and wherein 0.0001 mm < A_r and $\lambda_r \geq$ 0.0001 mm. In certain embodiments, the article is a rainproof product, 0.0001 mm < A_r and $\lambda_r \geq$ 0.0001 mm. In some embodiments, the article is a steam turbine blade, 0.00001 mm < A_r

and $\lambda_r > 0.0001$ mm. In one embodiment, the article is an exterior aircraft part, 0.00001 mm $< A_r$ and $\lambda_r > 0.0001$ mm. The article may be a gas turbine blade with 0.00001 mm $< A_r$ and $\lambda_r > 0.0001$ mm.

[0012] In certain embodiments, the macro-scale features include protrusions having height A_p and whose centers are separated by a distance λ_p, with $A_p/h > 0.01$ and $\lambda_p/A_p \geq 2$, wherein h is lamella thickness upon droplet impingement onto the surface. In certain embodiments, $100 > A_p/h > 0.01$ and $\lambda_p/A_p \geq 2$. In one embodiment, $10 > A_p/h > 0.1$ and $\lambda_p/A_p \geq 2$. The macro-scale features may be hemispherical protrusions.

[0013] In certain embodiments, the article is a wind turbine blade, the macro-scale features include protrusions having height A_p and whose centers are separated by a distance λ_p, and wherein 0.0001 mm $< A_p$ and $\lambda_p \geq 0.0002$ mm. In certain embodiments, the article is a rainproof product, 0.0001 mm $< A_p$ and $\lambda_p \geq 0.0002$ mm. In various embodiments, the article is a steam turbine blade, 0.00001 mm $< A_p$ and $\lambda_p \geq 0.00002$ mm. In certain embodiments, the article is an exterior aircraft part, 0.00001 mm $< A_p$ and $\lambda_p \geq 0.00002$ mm. The article may be a gas turbine blade with 0.00001 mm $< A_p$ and $\lambda_p \geq 0.00002$ mm.

[0014] In certain embodiments, the macro-scale features include a sinusoidal profile having amplitude A_c and period λ_c, with $A_c/h > 0.01$ and $\lambda_c/A_c \geq 2$, wherein h is lamella thickness upon droplet impingement onto the surface. In certain embodiments, $100 > A_c/h > 0.01$ and $500 \geq \lambda_c/A_c \geq 2$. In various embodiments, $100 > A_c/h > 0.1$ and $500 \geq \lambda_c/A_c \geq 2$. As used herein, "sinusoidal" encompasses any curved shape with an amplitude and period.

[0015] In certain embodiments, the article is a rainproof product, the macro-scale features include a sinusoidal profile having amplitude A_c and period λ_c, and wherein 0.0001 mm $< A_c$ and $\lambda_c \geq 0.0002$ mm. In one embodiment, the article is a wind turbine blade, 0.0001 mm $< A_c$ and $\lambda_c \geq 0.0002$ mm. The article may be a steam turbine blade with 0.00001 mm $< A_c$ and $\lambda_c \geq 0.00002$ mm. The article may be an exterior aircraft part with 0.00001 mm $< A_c$ and $\lambda_c \geq 0.00002$ mm. In certain embodiments, the article is a gas turbine blade, 0.00001 mm $< A_c$ and $\lambda_c \geq 0.00002$ mm.

[0016] In certain embodiments, the surface includes an alkane. In one embodiment, the surface includes a fluoropolymer. In certain embodiments, the surface includes at least one member selected from the group consisting of teflon, trichloro(1H,1H,2H,2H-perfluorooctyl)silane (TCS), octadecyltrichlorosilane (OTS), heptadecafluoro- 1,1,2,2-tetrahydrodecyltrichlorosilane, fluoroPOSS, a ceramic material, a polymeric material, a fluorinated material, an intermetallic compound, and a composite material. In certain embodiments, the surface includes a polymeric material, the polymeric material including at

least one of polytetrafluoroethylene, fluoroacrylate, fluoroeurathane, fluorosilicone, fluorosilane, modified carbonate, chlorosilanes, and silicone. In certain embodiments, the surface includes a ceramic material, the ceramic material including at least one of titanium carbide, titanium nitride, chromium nitride, boron nitride, chromium carbide, molybdenum carbide, titanium carbonitride, electroless nickel, zirconium nitride, fluorinated silicon dioxide, titanium dioxide, tantalum oxide, tantalum nitride, diamond-like carbon, and fluorinated diamond-like carbon. In certain embodiments, the surface includes an intermetallic compound, the intermetallic compound including at least one of nickel aluminide and titanium aluminide. In certain embodiments, the article is a condenser. The article may be a drip shield for storage of radioactive material. In certain embodiments, the article is a self-cleaning solar panel.

[0017] In another aspect, the invention relates to an atomizer including a non-wetting surface having a dynamic contact angle of at least about 90°, said surface patterned with macro-scale features configured to induce controlled asymmetry in a liquid film produced by impingement of a droplet onto the surface, thereby promoting breakup of the droplet on the surface. The description of elements of the embodiments above can be applied to this aspect of the invention as well. In certain embodiments, the non-wetting surface is supermetallophobic. In certain embodiments, the droplet includes a molten metal.

Brief Description of the Drawings

[0018] The objects and features of the invention can be better understood with reference to the drawings described below, and the claims. The drawings are not necessarily to scale, emphasis instead generally being placed upon illustrating the principles of the invention. In the drawings, like numerals are used to indicate like parts throughout the various views.

[0019] While the invention is particularly shown and described herein with reference to specific examples and specific embodiments, it should be understood by those skilled in the art that various changes in form and detail may be made therein without departing from the spirit and scope of the invention.

[0020] FIG. 1a is a schematic side view of a droplet resting on a surface during a static contact angle measurement, according to an illustrative embodiment of the invention.

[0021] FIGS. 1b and 1c are schematic side views of a liquid spreading and receding, respectively, on a surface, according to an illustrative embodiment of the invention.

[0022] FIG. 1d is a schematic side view of a droplet resting on an angled surface, according to an illustrative embodiment of the invention.

[0023] FIGS. 1e and 1f depict typical side and top views, respectively, of a water droplet (2.7 mm in diameter) impinging a superhydrophobic surface, according to an illustrative embodiment of the invention.

[0024] FIG. 2a is a schematic top view of a droplet undergoing symmetrical recoil, similar to FIG. 1b, after impingement, according to an illustrative embodiment of the invention.

[0025] FIG. 2b is a schematic top view of a droplet undergoing asymmetric recoil due to nucleation of holes, according to an illustrative embodiment of the invention.

[0026] FIG. 2c is a schematic top view of a droplet undergoing asymmetrical recoil due to development of cracks, according to an illustrative embodiment of the invention.

[0027] FIG. 2d is a schematic side view of a droplet that has spread onto a curved surface to form a lamella, according to an illustrative embodiment of the invention.

[0028] FIG. 3 is a schematic side view and a detailed view of a surface for triggering cracks in a receding liquid film, according to an illustrative embodiment of the invention.

[0029] FIG. 4 includes schematic top and cross-sectional views of a droplet recoiling on a flat surface, according to an illustrative embodiment of the invention.

[0030] FIG. 5 includes schematic top and cross-sectional views of a droplet recoiling on a ridge, according to an illustrative embodiment of the invention.

[0031] FIGS. 6a-6c include top, cross-sectional, and high-magnification scanning electron microscope (SEM) images of a macro-scale ridge (height ~ 150 μm, width ~ 200μm) fabricated on a silicon wafer using laser-rastering, according to an illustrative embodiment of the invention.

[0032] FIG. 6d includes high-speed photography images of droplet impingement on the ridge of FIGS. 6a-6c, according to an illustrative embodiment of the invention.

[0033] FIG. 7a is an SEM image of a macro-scale ridge (height ~ 100 μm, width ~ 200μm) milled on an anodized aluminum oxide (AAO) surface, according to an illustrative embodiment of the invention.

[0034] FIG. 7b is a high-magnification SEM image of the AAO surface of FIG. 7a, showing nanoscale pores, according to an illustrative embodiment of the invention.

[0035] FIG. 7c includes high-speed photography images of droplet impingement on the ridge of FIG. 7a, according to an illustrative embodiment of the invention.

[0036] FIG. 8 is a schematic perspective view of macro-scale protrusions on a surface, according to an illustrative embodiment of the invention.

[0037] FIG. 9a is an SEM image of macro-scale protrusions (~ 50-100 μm) fabricated on anodized titanium oxide (ATO) surface, according to an illustrative embodiment of the invention.

[0038] FIG. 9b is a high-magnification SEM image of the ATO surface of FIG. 9a showing nanoscale features, according to an illustrative embodiment of the invention.

[0039] FIG. 9c includes high-speed photography images of droplet impingement on the surface of FIG. 9a, according to an illustrative embodiment of the invention.

[0040] FIG. 10 includes a schematic cross-sectional view and a detailed schematic cross-sectional view of a surface having a macro-scale sinusoidal profile to trigger curvature in a receding liquid film, according to an illustrative embodiment of the invention.

[0041] FIG. 11a includes a photograph showing a macro-scale sinusoidal surface fabricated on silicon and an image showing high magnification SEM sub-micron features, according to an illustrative embodiment of the invention.

[0042] FIG. 11b includes high-speed photography images of droplet impingement on the surface of FIG. 11a, according to an illustrative embodiment of the invention.

[0043] FIG. 12a is a schematic view of droplet impingement on a solid surface at the instant of impact, according to an illustrative embodiment of the invention.

[0044] FIG. 12b is a schematic view of droplet impingement on a solid surface during spreading, according to an illustrative embodiment of the invention.

[0045] FIG. 12c is a schematic view of droplet impingement on a solid surface at the instant when spreading comes to a rest, according to an illustrative embodiment of the invention.

Detailed Description

[0046] It is contemplated that compositions, mixtures, systems, devices, methods, and processes of the claimed invention encompass variations and adaptations developed using information from the embodiments described herein. Adaptation and/or modification of the compositions, mixtures, systems, devices, methods, and processes described herein may be performed by those of ordinary skill in the relevant art.

[0047] Throughout the description, where devices and systems are described as having, including, or comprising specific components, or where processes and methods are described as having, including, or comprising specific steps, it is contemplated that, additionally, there are systems of the present invention that consist essentially of, or consist of, the recited

components, and that there are processes and methods according to the present invention that consist essentially of, or consist of, the recited processing steps.

[0048] Similarly, where devices, mixtures, and compositions are described as having, including, or comprising specific compounds and/or materials, it is contemplated that, additionally, there are mixtures and compositions of the present invention that consist essentially of, or consist of, the recited compounds and/or materials.

[0049] It should be understood that the order of steps or order for performing certain actions is immaterial so long as the invention remains operable. Moreover, two or more steps or actions may be conducted simultaneously.

[0050] The mention herein of any publication, for example, in the Background section, is not an admission that the publication serves as prior art with respect to any of the claims presented herein. The Background section is presented for purposes of clarity and is not meant as a description of prior art with respect to any claim.

[0051] Referring to FIG. 1a, in certain embodiments, a static contact angle θ between a liquid and solid is defined as the angle formed by a liquid drop 12 on a solid surface 14 as measured between a tangent at the contact line, where the three phases – solid, liquid, and vapor – meet, and the horizontal. The term "contact angle" usually implies the *static* contact angle θ since the liquid is merely resting on the solid without any movement.

[0052] As used herein, dynamic contact angle, θ_d, is a contact angle made by a *moving* liquid 16 on a solid surface 18. In the context of droplet impingement, θ_d may exist during either advancing or receding movement, as shown in FIGS. 1b and 1c, respectively.

[0053] As used herein, a surface is "non-wetting" if it has a dynamic contact angle with a liquid of at least 90 degrees. Examples of non-wetting surfaces include, for example, superhydrophobic surfaces and superoleophobic surfaces.

[0054] As used herein, contact angle hysteresis (CAH) is

$$CAH = \theta_a - \theta_r \tag{2}$$

where θ_a and θ_r are advancing and receding contact angles, respectively, formed by a liquid 20 on a solid surface 22. Referring to FIG. 1d, the advancing contact angle θ_a is the contact angle formed at the instant when a contact line is about to advance, whereas the receding contact angle θ_r is the contact angle formed when a contact line is about to recede.

[0055] As used herein, "non-wetting features" are physical textures (e.g., random, including fractal, or patterned surface roughness) on a surface that, together with the surface

chemistry, make the surface non-wetting. In certain embodiments, non-wetting features result from chemical, electrical, and/or mechanical treatment of a surface. In certain embodiments, an intrinsically hydrophobic surface may become superhydrophobic when non-wetting features are introduced to the intrinsically hydrophobic surface. Similarly, an intrinsically oleophobic surface may become superoleophobic when non-wetting features are introduced to the intrinsically oleophobic surface. Likewise, an intrinsically metallophobic surface may become supermetallophobic when non-wetting features are introduced to the intrinsically metallophobic surface.

[0056] In certain embodiments, non-wetting features are micro-scale or nano-scale features. For example, the non-wetting features may have a length scale L_n (e.g., an average pore diameter, or an average protrusion height) that is less than about 100 microns, less than about 10 microns, less than about 1 micron, less than about 0.1 microns, or less than about 0.01 microns. Compared to a length scale L_m associated with macro-scale features, described herein, the length scales for the non-wetting features are typically at least an order of magnitude smaller. For example, when a surface includes a macro-scale feature that has a length scale L_m of 1 micron, the non-wetting features on the surface have a length scale L_n that is less than 0.1 microns. In certain embodiments a ratio of the length scale for the macro-scale features to the length scale for the non-wetting features (i.e., L_m / L_n) is greater than about 10, greater than about 100, greater than about 1000, or greater than about 10,000.

[0057] As used herein, a "superhydrophobic" surface is a surface having a static contact angle with water of at least 120 degrees and a CAH of less than 30 degrees. In certain embodiments, an intrinsically hydrophobic material (i.e., a material having an intrinsic contact angle with water of at least 90 degrees) exhibits superhydrophobic properties when it includes non-wetting features. For superhydrophobicity, typically nano-scale non-wetting features are preferred. Examples of intrinsically hydrophobic materials that exhibit superhydrophobic properties when given non-wetting features include: hydrocarbons, such as alkanes, and fluoropolymers, such as teflon, trichloro(1H,1H,2H,2H-perfluorooctyl)silane (TCS), octadecyltrichlorosilane (OTS), heptadecafluoro- 1,1,2,2-tetrahydrodecyltrichlorosilane, and fluoroPOSS.

[0058] As used herein, a "superoleophobic" surface is a surface having a static contact angle with oil of at least 120 degrees and a CAH with oil of less than 30 degrees. The oil may be, for example, a variety of liquid materials with a surface tension much lower than the surface tension of water. Examples of such oils include alkanes (e.g., decane, hexadecane, octane), silicone oils, and fluorocarbons. In certain embodiments, an intrinsically oleophobic

material (i.e., a material having an intrinsic contact angle with oil of at least 90 degrees) exhibits superoleophobic properties when it includes non-wetting features. The non-wetting features may be random or patterned. Examples of intrinsically oleophobic materials that exhibit superoleophobic properties when given non-wetting features include: teflon, trichloro(1H,1H,2H,2H-perfluorooctyl)silane (TCS), octadecyltrichlorosilane (OTS), heptadecafluoro- 1,1,2,2-tetrahydrodecyltrichlorosilane, fluoroPOSS, and other fluoropolymers.

[0059] As used herein, a "supermetallophobic" surface is a surface having a static contact angle with a liquid metal of at least 120 degrees and a CAH with liquid metal of less than 30 degrees. In certain embodiments, an intrinsically metallophobic material (i.e., a material having an intrinsic contact angle with liquid metal of at least 90 degrees) exhibits supermetallophobic properties when it includes non-wetting features. The non-wetting featuers may be random or patterned. Examples of intrinsically metallophobic materials that exhibit supermetallophobic properties when given non-wetting features include: teflon, trichloro(1H,1H,2H,2H-perfluorooctyl)silane (TCS), octadecyltrichlorosilane (OTS), heptadecafluoro- 1,1,2,2-tetrahydrodecyltrichlorosilane, fluoroPOSS, and other fluoropolymers. Examples of metallophobic materials include molten tin on stainless steel, silica, and molten copper on niobium.

[0060] In certain embodiments, intrinsically hydrophobic materials and/or intrinsically oleophobic materials include ceramics, polymeric materials, fluorinated materials, intermetallic compounds, and composite materials. Polymeric materials may include, for example, polytetrafluoroethylene, fluoroacrylate, fluoroeurathane, fluorosilicone, fluorosilane, modified carbonate, chlorosilanes, silicone, and/or combinations thereof. Ceramics may include, for example, titanium carbide, titanium nitride, chromium nitride, boron nitride, chromium carbide, molybdenum carbide, titanium carbonitride, electroless nickel, zirconium nitride, fluorinated silicon dioxide, titanium dioxide, tantalum oxide, tantalum nitride, diamond-like carbon, fluorinated diamond-like carbon, and/or combinations thereof. Intermetallic compounds may include, for example, nickel aluminide, titanium aluminide, and/or combinations thereof.

[0061] As used herein, an intrinsic contact angle is a static contact angle formed between a liquid and a perfectly flat, ideal surface. This angle is typically measured with a goniometer. The following publications, which are hereby incorporated by reference herein in their entireties, describe additional methods for measuring the intrinsic contact angle: C. Allain, D. Aussere, and F. Rondelez, *J. Colloid Interface Sci.*, 107, 5 (1985); R. Fondecave, and F.

Brochard-Wyart, *Macromolecules*, 31, 9305 (1998); and A. W. Adamson, *Physical Chemistry of Surfaces* (New York: John Wiley & Sons, 1976).

[0062] When a liquid droplet impacts a non-wetting surface, the droplet will spread out on the surface and then begin to recoil. For highly non-wetting surfaces, the droplet can completely rebound from the surface. Through the impact dynamics, the shape of the droplet is generally axisymmetric so that, at any point in time during recoil, the wetted area is substantially circular. By patterning the surface, however, this symmetry may be disrupted and the impact dynamics may be altered or controlled. For example, by controlling or defining macro-scale features on the surface, the contact time of the droplet may be increased or decreased, instabilities may be created that cause the droplet to break-up into smaller droplets, and spatial control may be gained over how long a particular drop, or part of that drop, is in contact with the surface.

[0063] During the time of contact between a droplet and a surface, heat, mass, and momentum diffuse between the droplet and the surface. By controlling the time that a droplet contacts a particular location on the surface, this diffusion may be optimized both temporally and spatially. In certain embodiments, surface patterns or features are developed that influence the recoil of droplets in two distinct ways: (1) patterns that introduce concavity to the receding boundary, and (2) patterns that introduce surface curvature to the film in such a way that capillary pressure delaminates the spread-out droplet from the surface.

[0064] The speed at which a spread-out droplet recedes depends not only on the material properties of the droplet, but also the properties of the surface the droplet contacts. On non-wetting surfaces, the drop recoiling speed is reduced by the dissipation or contact angle hysteresis from the surface. Variations in dissipation may be achieved by changing the structure and/or chemistry of the surface patterns that form the non-wetting surface. For example, the density of patterns such as posts can influence the recoiling speed of drops. Dissipation in the system may be added using a variety of tools, such as flexible structures at various length scales. In addition, while a pattern of posts can break the symmetry of receding films, the drops may remain convex.

[0065] In certain embodiments, surfaces are designed that introduce concavity into the receding film. Using these designs, the surfaces are tailored so that the exposure to droplets in certain regions is longer than it is in other regions. In one embodiment, concavity breaks the film into separate drops, and the concavity is augmented by natural capillary instabilities. For example, the surface may be patterned so the recoil of the drop in one direction is significantly slower than in a perpendicular direction. The resulting recoil forms a cylinder

which quickly becomes concave and breaks up into droplets via a Rayleigh-Plateau type instability.

[0066] A limitation in the surface pinning approach is that it may slow down the drop dynamics. The minimum contact time a drop makes with a surface is believed to be minimized when that surface approaches a 180 degree contact angle with no contact angle hysteresis, the equivalent of impacting on a thin air layer. As described herein, however, a shorter contact time is possible using patterned surfaces. Specifically, if during the recoiling stage, the contact line increases while the surface area decreases, there are more fronts on which the droplet can recoil. It is therefore possible for the drop to recede more quickly than if the drop were receding symmetrically, so that the total contact time for the drop is reduced. As described below, in certain embodiments, concavity is introduced by speeding up the recoil of portions of the receding film.

[0067] FIGS. 1a and 1b depict side and top views, respectively, of a water droplet 100 bouncing on a superhydrophobic surface 102. The surface 102 includes an array of 10 μm square posts of silicon spaced 3 μm apart. The contact time in this case, measured from the leftmost image to the rightmost in these figures, is about 19 ms. The scale bar 104 in the leftmost image of FIG. 1a is 3 mm. FIG. 1b shows that the droplet spreads and recedes with a largely symmetrical (circular) edge 106.

[0068] In certain embodiments, the devices and methods presented herein reduce the contact time between an impinging droplet and a surface by modifying surface textures associated with the surface. Surprisingly, these devices and methods reduce the contact time to below the theoretical limit indicated by Equation 1, above. In one embodiment, by appropriately designing the superhydrophobic surface, contact times are further decreased to about one half of this theoretical limit.

[0069] In certain embodiments, the devices and methods described herein incorporate macro-scale features (e.g., ridges, sinusoids, protrusions) into a superhydrophobic surface to trigger controlled asymmetry in the liquid film produced by droplet impingement. The macro-scale features may have, for example, a height greater than about 0.00001 mm, greater than about 0.0001 mm, greater than about 0.001 mm, greater than about 0.01 mm, greater than about 0.1 mm, or greater than about 1 mm. Additionally, the macro-scale features may have, for example, a spacing (e.g., a spacing between ridges, peaks, or valleys) greater than about 0.00001 mm, greater than about 0.0001 mm, greater than about 0.001 mm, greater than about 0.01 mm, greater than about 0.1 mm, or greater than about 1 mm.

[0070] Referring to FIGS. 2a-2d, the asymmetry in a liquid film 200, in the form of cracks 204, holes 202, and curvature, introduced by the macro-scale features, leads to droplet recoiling at multiple fronts and, hence, produces a significant reduction in the contact time. This idea is distinctly different from previous approaches which typically included smaller features (e.g., 100 nm) and, more importantly, attempted to minimize the contact line pinning between the drop and these features.

[0071] In one embodiment, a superhydrophobic surface 300 includes macro-scale ridges 302 that trigger cracks in a liquid film upon impingement of a droplet having radius R. As depicted in FIG. 3, the ridges 302 have a ridge height A_r and a ridge spacing λ_r. The ridges 302 may have any cross-sectional shape, including curved and pointed (as shown in FIG. 3), triangular, hemispherical, and/or rectangular. Typically, each ridge 302 has a ridge length (along the surface 300) that is much greater than the ridge height A_r and/or ridge spacing λ_r. For example, a ridge 302 may have a ridge height A_r of about 0.1 mm and a ridge length (e.g., along a ridge longitudinal axis) of about 100 mm or more. To achieve or maintain superhydrophobicity, the surface 300 includes non-wetting features 304 having a length scale L_n (e.g., an average diameter or cross-dimension). In certain embodiments, the non-wetting features 304 are chosen so that θ_d is greater than 90 degrees and CAH is less than about 30 degrees, less than about 20 degrees, or less than about 10 degrees. As depicted, the non-wetting features may include smaller features 306, if necessary, to facilitate non-wetting.

[0072] Referring again to FIGS. 1b and 1c, when a liquid droplet impinges a solid surface, the droplet spreads into a thin lamella or film having a thickness h. In certain embodiments, a ratio of the ridge height A_r to the thickness h (i.e., A_r/h) is greater than about 0.01. For example, A_r/h may be from about 0.01 to about 100, from about 0.1 to about 10, or from about 0.1 to about 5. In certain embodiments, a ratio of the ridge spacing λ_r to the ridge height A_r is greater than or equal to about 1.

[0073] FIGS. 4 and 5 are schematic diagrams showing a droplet 400 recoiling on a flat surface 402 and a droplet 500 recoiling on a ridge 502, respectively. As depicted, on the flat surface 402 of FIG. 4, droplet recoil is typically symmetric, with the droplet 400 remaining substantially circular over time. By comparison, on the ridge 502 of FIG. 5, droplet recoil is asymmetric, with thinner portions 504 (having thickness h_1) at the ridge 502 recoiling faster than thicker portions 506 (having thickness h_2) adjacent to the ridge 502. The thinner portions 504 may be referred to as cracks. As depicted, the ridges 502 create cracks or pathways that promote droplet fracture. These pathways cause the contact line to penetrate

into the droplet 500 along the ridge 502, thereby increasing the contact line length during droplet recoil and reducing contact time.

[0074] FIGS. 6a-6d and 7a-7c depict experimental examples of surfaces for triggering cracks in a liquid film upon droplet impingement, in accordance with certain embodiments of the invention. FIGS. 6a-6d show photographs of droplet impingement on a ridge 600 fabricated on a silicon surface 602 using laser-rastering. FIGS. 7a-7c show droplet impingement on a ridge 700, of similar dimensions, milled on an aluminum surface 702, followed by anodization to create nano-scale pores. Both surfaces 602, 702 were made superhydrophobic by depositing trichloro(1H,1H,2H,2H-perfluorooctyl)silane. The diameter of the droplet before impingement was 2.6 mm (i.e., R=1.3 mm) and the impact velocity was 1.8 m/s.

[0075] FIGS. 6a-6c show the details of the silicon surface 602 with the help of SEM images of the ridge 600, which had a ridge height A_r of about 150 μm and width W of about 200μm. These figures also show the non-wetting features achieved to maintain superhydrophobicity. The dynamics of droplet impingement are shown in Fig. 6d, which reveals that a droplet 604 deforms asymmetrically and develops a crack 606 along the ridge 600. The crack 606 creates additional recoiling fronts which propagate rapidly along the ridge 600 until the film is split into multiple drops 608. The contact time in this case was only 7 ms – almost one-third of the contact time for the example shown in FIG. 1, and about 50% less than the theoretical prediction from Equation 1 (i.e., 13.5 ms) with $\phi = 0$.

[0076] As mentioned above, the ridges may have any cross-sectional shape, including the approximately rectangular cross-section depicted in FIG. 6a. Additionally, a ratio of the ridge height A_r to the width W (i.e., A_r/W) may be, for example, from about 0.1 to about 10.

[0077] FIGS. 7a-7c show similar contact time reduction achieved on the anodized aluminum oxide (AAO) surface 702. The contact time in this case was about 6.3 ms, which is over 50% smaller than the theoretical prediction of Equation 1 (i.e., 13.5 ms). The details of the surface 702 are shown in FIGS. 7a and 7b with the help of SEM images revealing the ridge texture and the nanoporous structure. The scale bars 704, 706 in FIGS. 7a and 7b are 100 μm and 1 μm, respectively. Referring to FIG. 7c, the dynamics of droplet impingement show behavior similar to that seen on the laser-rastered silicon surface. For example, a droplet 708 deforms asymmetrically with a crack 710 developing along the ridge 700, thereby causing the liquid film to recoil rapidly along the ridge 700 and split into multiple drops 712.

[0078] In certain embodiments, the reduction of contact time, as shown in the examples in FIGS. 6a-6d through 7a-7c, is more a result of surface design or structure, rather than the surface material or other surface property. For example, although the surfaces in these examples were produced by completely different methods (i.e., laser-rastering in FIG. 6a-6d, and milling and anodizing in FIGS. 7a-7c), the similar macro-scale features (e.g., ridge size and shape) of the two surfaces resulted in similar drop impingement dynamics.

[0079] In another embodiment, a superhydrophobic surface 800 includes macro-scale protrusions 802 that nucleate holes in a liquid film upon impingement of a droplet having radius R. The protrusions 802 may have any shape, including spherical, hemispherical, dome-shaped, pyramidal, cube-shaped, and combinations thereof. For example, in the embodiment depicted in FIG. 8, the protrusions 802 are substantially dome-shaped with a protrusion height A_p and are spaced in grid with a protrusion spacing λ_p. To achieve or maintain superhydrophobicity, the surface 800 includes non-wetting features having a length scale L_n. As mentioned above, the non-wetting features are chosen so that θ_d is greater than 90 degrees and CAH is less than about 30 degrees, less than about 20 degrees, or less than about 10 degrees.

[0080] In certain embodiments, a ratio of the protrusion height A_p to the lamella or film thickness h (i.e., A_p/h) is greater than or equal to about 0.01. For example, A_p/h may be from about 0.01 to about 100, or from about 0.1 to about 10, or from about 0.1 to about 3. In certain embodiments, a ratio of the protrusion spacing λ_p to the protrusion height A_p (i.e., λ_p/A_p) is greater than or equal to about 2.

[0081] FIGS. 9a-9c depict an example surface 900 that includes macro-scale protrusions 902 for nucleating a droplet upon impingement. The surface 900 in this example is made of anodized titanium oxide (ATO). Details of the surface 900 are shown in the SEM images. The scale bars 904, 906 in FIGS. 9a and 9b are 100 μm and 4 μm, respectively. As depicted, the surface includes macro-scale protrusions 902, of about 20-100μm, which further contain non-wetting features to maintain superhydrophobicity. Referring to the highspeed photography images in FIG. 9c, after a droplet 908 impinges the ATO surface (at t = 0), the droplet 908 spreads into a thin film (at t = 2 ms) that destablizes internally and nucleates into several holes 910 (at t = 4 ms). The holes 910 grow until their boundaries meet or collide, thereby causing fragmentation of the entire film. Each hole 910 creates additional fronts where the film may recoil, thus resulting in a significant reduction in contact time. The

contact time in this example was about 8.2 ms, which is again much smaller than the theoretical prediction (i.e., 13.5 ms) from Equation 1 with $\phi = 0$.

[0082] In the depicted embodiments, the protrusions increase the contact line of the droplet by introducing holes in the droplet. The holes increase or open during recoil, thereby reducing the contact time.

[0083] In another embodiment, a superhydrophobic surface 1000 includes macro-scale curved profiles 1002 that introduce curvature in a liquid film upon impingement of a droplet having radius R. The curved profiles 1002 may have any shape, including sinusoidal and/or parabolic (e.g., piece-wise). Compared to the ridges 302 and protrusions 802, described above, the curved profiles 1002 are generally smoother, with less abrupt variations in surface height. For example, in the embodiment depicted in FIG. 10, the curved profiles 1002 define a sinusoidal pattern of peaks and valleys on the surface. The sinusoidal pattern has a wave amplitude A_c and a wave spacing λ_c (i.e., the distance from a peak to a valley). The wave spacing λ_c may also be referred to as half the period of the sinusoidal pattern.

[0084] In certain embodiments, the surface 1000 includes curvature along more than one direction. For example, a height of surface 1000 may vary sinusoidally along one direction and sinusoidally along another, orthogonal direction.

[0085] To achieve or maintain superhydrophobicity, the surface 1000 includes non-wetting features having a length scale L_n. As mentioned above, the non-wetting features are chosen so that θ_d is greater than 90 degrees and CAH is less than about 30 degrees, less than about 20 degrees, or less than about 10 degrees.

[0086] In certain embodiments, a ratio of the wave amplitude A_c to the thickness h (i.e., A_c/h) is greater than or equal to about 0.01. For example, A_c/h may be from about 0.01 to about 100, or from about 0.1 to about 100, or from about 0.1 to about 50, or from about 0.1 to about 9. In certain embodiments, a ratio of the wave spacing λ_c to the wave amplitude A_c (i.e., λ_c/A_c) is greater than or equal to about 2. For example, λ_c/A_c may be from about 2 to about 500, or from about 2 to about 100.

[0087] FIG. 11a depicts an example of a sinusoidal curved surface 1100 fabricated on silicon using laser rastering. The details of the surface 1100 are shown with the help of SEM images. The wave amplitude A_c of the sinusoidal pattern was about 350 μm while its period (i.e., twice the wave spacing λ_c) was 2 mm. The surface 1100 was made superhydrophobic by depositing trichloro(1H,1H,2H,2Hperfluorooctyl)silane. Referring to FIG. 11b, the dynamics of droplet impingement on the surface 1100 reveal that a droplet 1102 adopts the

curved profile of the surface 1100 while spreading and becomes a thin film of varying thickness. The film thickness is smallest at a crest or peak 1104 of the sinusoidal surface 1100 where the film recedes fastest, thereby causing the film to split across the crest 1104 and break into multiple drops 1106. The contact time in this example was only about 6 ms, which is again well over 50% smaller than the theoretical prediction of Equation 1 (i.e., 13.5 ms).

[0088] As described above with respect to FIGS. 10, 11a, and 11b, in certain embodiments, the contact time of the drop is reduced by controlling the local curvature of the surface. If the surface is curved so that part of the film covers a concave region, one of two scenarios may occur – both of which decrease the total contact time of the film on the surface. In one scenario, the film spreads over the concavity so that the thickness is nearly uniform. If the film is making contact with the curved surface, then the film is also curved, in which case the film curvature, along with surface tension, causes a pressure gradient that lifts the film off of the surface as quickly as the edges recoil. In the other scenario, the film spreads over the concavity in a way that the film surface is flat (i.e., not curved). In this case the film thickness is not uniform and, along contours where the film is thinner, the drop recoils more quickly than along areas where the film is thicker. As discussed above, by forming a hybrid surface of linked concave cusps, the contact time may be reduced below the theoretical limit defined by Equation 1.

[0089] When a liquid droplet 1200 of diameter D_o impinges a solid surface 1202 with velocity V_o, the droplet 1200 spreads into a thin lamella (film) 1204 of thickness h, eventually reaching a maximum diameter D_{max}, as shown in FIGS. 12a, 12b, and 12c. h can be estimated by applying mass conservation at the spherical droplet state, shown in FIG. 12a, and the lamella state, shown in FIG. 12c, with the assumptions that there is negligible mass loss (e.g., due to splashing or evaporation) during spreading and the lamella 1204 is substantially uniform in thickness in time and space, on average. With these assumptions, the mass of the droplet 1200 when equated at the spherical droplet state and the lamella state yields:

$$\rho\frac{\pi}{6}D_o^3 = \rho\frac{\pi}{4}D_{\max}^2 h\,, \tag{3}$$

where ρ is the density of droplet liquid. Solving Equation 3 for h gives:

$$h = \frac{2D_o}{3\xi_{\max}^2}\,, \tag{4}$$

where $\xi_{\max} = D_{\max} / D_o$ is the maximum spread factor of the impinging droplet. To calculate $\xi_{\max}$, an energy balance model may be used. According to this model, ξ_{max} is given as:

$$\xi_{\max} = \sqrt{\frac{We + 12}{3(1 - \cos\theta_a) + 4(We/\sqrt{\mathrm{Re}})}}, \quad (5)$$

where θ_a is the advancing contact angle formed by a droplet of liquid on the solid surface 1202, $We = \rho V_o^2 D_o / \gamma$ is the droplet Weber number, and $\mathrm{Re} = \rho V_o D_o / \mu$ is the droplet Reynolds number before impingement. Here γ and μ are the surface tension and dynamic viscosity of the droplet liquid, respectively. Equation 5 can be simplified further by approximating the value of expression $3(1 - \cos\theta_a)$ to 6 as θ_a, at maximum, can be 180°. With this simplification, Equation 5 becomes:

$$\xi_{\max} = \sqrt{\frac{We + 12}{6 + 4(We/\sqrt{\mathrm{Re}})}}, \quad (6)$$

Thus, once ξ_{max} is calculated from Equation 6, h can be estimated using Equation 4.

[0090] The devices and methods described herein have a wide range of applications, including rainproof products, wind turbines, steam turbine blades, aircraft wings, and gas turbine blades. Table 1 presents typical droplet radius values for several of these applications. As indicated, for rainproof products and wind turbine applications, droplet radius values may be from about 0.1 mm to about 5 mm. Similarly, for steam turbine blades, aircraft icing, and gas turbine blade applications, droplet radius values may be from about 0.01 mm to about 5 mm. In one embodiment, for rainproof products and wind turbine applications, lamella thickness values are from about 0.01 mm to about 1 mm, and ξ_{max} values are from about 5 to about 100. In another embodiment, for steam turbine blades, aircraft icing, and gas turbine blade applications, lamella thickness values are from about 0.001 mm to about 1 mm, and ξ_{max} values are from about 10 to about 500.

[0091] In certain embodiments, Table 1 is used to identify appropriate dimensions for the features described above (i.e., ridges, protrusions, and curved profiles) for reducing the contact time between an impinging droplet and a surface. For example, referring to Table 1, if the intended application is rainproof products and the feature type is ridges, then appropriate feature dimensions (in mm) are $0.0001 < A_r$ and $\lambda_r \geq 0.0001$. Likewise, if the intended application is gas turbine blades and the feature type is protrusions, then appropriate feature dimensions (in mm) are $0.00001 < A_p$ and $\lambda_p \geq 0.00002$.

[0092] As indicated in Table 1, A_r, A_p, or A_c may be greater than 0.00001 mm, and λ_r, λ_p, or λ_c may be greater than or equal to about 0.00001 mm. In certain embodiments, A_r, A_p, or A_c is greater than about 0.0001 mm, greater than about 0.001 mm, greater than about 0.01 mm, greater than about 0.1 mm, or greater than about 1 mm. In certain embodiments, A_r, A_p, or A_c is from about 0.00001 mm to about 0.001 mm, from about 0.0001 mm to about 0.01 mm, from about 0.001 mm to about 0.1 mm, or from about 0.01 mm to about 1 mm. In certain embodiments, λ_r, λ_p, or λ_c is greater than about 0.0001 mm, greater than about 0.001 mm, greater than about 0.01 mm, greater than about 0.1 mm, or greater than about 1 mm. In certain embodiments, λ_r, λ_p, or λ_c is from about 0.00001 mm to about 0.001 mm, from about 0.0001 mm to about 0.01 mm, from about 0.001 mm to about 0.1 mm, or from about 0.01 mm to about 1 mm.

Application	**Droplet Radius, *R* (mm)**	**Impact Velocity, *V* (m/s)**	**Lamella Thickness, *h* (mm)**	**Feature Type**	**Feature Dimensions* (mm)**
Rainproof products & wind turbine	0.1-5	0.5-20	0.01-1	Type (i): ridges	$0.0001 < A_r$, $\lambda_r \geq 0.0001$
				Type (ii): protrusions	$0.0001 < A_p$, $\lambda_p \geq 0.0002$
				Type (iii): curvature	$0.0001 < A_c$, $0.0002 \leq \lambda_c$
Steam turbine blades, Aircraft icing, Gas turbine blades	0.01-5	0.5-200	0.001-1	Type (i): ridges	$0.00001 < A_r$, $\lambda_r > 0.00001$
				Type (ii): protrusions	$0.00001 < A_p$, $\lambda_p \geq 0.00002$
				Type (iii): curvature	$0.00001 < A_c$, $0.00002 \leq \lambda_c$

Table 1. Ranges for droplet radius and macro-scale feature dimensions.

[0093] In alternative embodiments, the devices and methods described herein apply to droplets of oil-based liquids impinging on an oleophobic surface or a superoleophobic

surface. In this case, the macro-scale features, such as ridges, protrusions, and sinusoidal patterns, may produce oil droplet impingement dynamics that are similar to those shown and described for water droplets impinging a hydrophobic or superhydrophobic surface.

[0094] In certain embodiments, when a water droplet impinges a surface that is hot enough to vaporize the liquid quickly and generate sufficient pressure, the droplet can spread and rebound without ever touching the surface, mimicking a situation seen in superhydrophobic surfaces. This so-called Leidenfrost phenomenon is an example of a non-wetting situation without the surface being superhydrophobic. In one embodiment, the macro-scale features applied to this type of surface are effective in reducing the contact time of an impinging droplet. Specifically, the droplet dynamics are similar to those described above for the superhydrophobic surfaces, and the contact time reduction is of similar magnitude (~ 50% of the theoretical limit). In one embodiment, to achieve the desired non-wetting behavior, the surface is heated to a temperature greater than the Leidenfrost temperature.

[0095] Blades of steam and gas turbines are sometimes fouled by metallic fragments that are produced due to erosion/corrosion of intermediary equipment in the power cycle. These fragments are carried along with the working fluid (steam or combustion gases, as the case may be) and melt when they reach regions of high temperatures. The melted liquid impinges upon turbine blades and gets stuck thereby deteriorating aerodynamical performance and hence turbine power output. Our surface designs can solve this problem by rapidly repelling the impinging molten liquid before it can freeze on blade surfaces.

Experimental Examples

[0096] As described herein, a series of experiments were conducted to measure and visualize the impingement of droplets on surfaces having macro-scale features. A high speed camera system (Model SA 1.1, PHOTRON USA, San Diego, CA) was utilized to capture a sequence of images of the droplet impingement. Droplets of controlled volume (10 μL) were dispensed using a syringe pump (HARVARD APPARATUS, Holliston, MA) using a 26 gauge stainless steel needle. Droplet impact velocity was controlled by setting the needle at a certain height (150 mm) above the surface. Contact times were determined from the images by identifying the time difference between the point of initial droplet contact with the surface and the subsequent rebound of liquid from the surface.

[0097] Images of macro-scale ridges and droplets impinging on the ridges are provided in FIGS. 6a-6d and 7a-7c, in accordance with certain embodiments of the invention. FIGS. 6a-6d show photographs of droplet impingement on a ridge 600 fabricated on a silicon surface 602 using laser-rastering. FIGS. 7a-7c show droplet impingement on a ridge 700, of similar

dimensions, milled on an aluminum surface 702, followed by anodization to create nano-scale pores. Both surfaces 602, 702 were made superhydrophobic by depositing trichloro(1H,1H,2H,2H-perfluorooctyl)silane. The diameter of the droplet before impingement was 2.6 mm (i.e., R=1.3 mm) and the impact velocity was 1.8 m/s. As discussed in detail above, the contact times achieved with the macro-scale ridges were about 50% less than the theoretical prediction from Equation 1 (i.e., 13.5 ms) with $\phi = 0$.

[0098] Images of macro-scale protrusions and droplets impinging on the protrusions are provided in FIGS. 9a-9c, in accordance with certain embodiments of the invention. The surface 900 in this example is made of anodized titanium oxide (ATO). Details of the surface 900 are shown in the SEM images. The scale bars 904, 906 in FIGS. 9a and 9b are 100 μm and 4 μm, respectively. As depicted, the surface includes macro-scale protrusions 902, of about 20-100μm, which further contain non-wetting features to maintain superhydrophobicity. As discussed in detail above, the contact times achieved with the macro-scale protrusions was about half of the theoretical prediction (i.e., 13.5 ms) from Equation 1 with $\phi = 0$.

[0099] Images of macro-scale curvature and droplets impinging on the curvature are provided in FIGS. 11a and 11b, in accordance with certain embodiments of the present invention. As discussed above, the sinusoidal curved surface 1100 was fabricated on silicon using laser rastering. The details of the surface 1100 are shown with the help of SEM images. The wave amplitude A_c of the sinusoidal pattern was about 350 μm while its period (i.e., twice the wave spacing λ_c) was 2 mm. The surface 1100 was made superhydrophobic by depositing trichloro(1H,1H,2H,2Hperfluorooctyl)silane. The contact time in this example was only about 6 ms, which is again well over 50% smaller than the theoretical prediction of Equation 1 (i.e., 13.5 ms).

Equivalents

[00100] While the invention has been particularly shown and described with reference to specific preferred embodiments, it should be understood by those skilled in the art that various changes in form and detail may be made therein without departing from the spirit and scope of the invention as defined by the appended claims.

[00101] What is claimed is:

1. An article comprising a non-wetting surface having a dynamic contact angle of at least about 90°, said surface patterned with macro-scale features configured to induce controlled asymmetry in a liquid film produced by impingement of a droplet onto the surface, thereby reducing time of contact between the droplet and the surface.

2. The article of claim 1, wherein the non-wetting surface is superhydrophobic.

3. The article of claim 1, wherein the non-wetting surface is superoleophobic.

4. The article of claim 1, wherein the non-wetting surface is supermetallophobic.

5. The article of any one of claims 1-4, wherein the surface comprises a non-wetting material.

6. The article of any one of claims 1-5, wherein the surface comprises non-wetting features.

7. The article of claim 6, wherein the non-wetting features are nanoscale pores.

8. The article of any one of the preceding claims, wherein the surface is heated above its Leidenfrost temperature.

9. The article of any one of the preceding claims, wherein the macro-scale features comprise ridges having height A_r and spacing λ_r, with A_r/h greater than about 0.01 and λ_r/A_r greater than or equal to about 1, wherein h is lamella thickness upon droplet impingement onto the surface.

10. The article of any one of the preceding claims, wherein the macro-scale features comprise ridges having height A_r and spacing λ_r, with A_r/h from about 0.01 to about 100 and λ_r/A_r greater than or equal to about 1, wherein h is lamella thickness upon droplet impingement onto the surface.

11. The article of any one of the preceding claims, wherein the macro-scale features comprise ridges having height A_r and spacing λ_r, with A_r/h from about 0.1 to about 10 and λ_r/A_r greater than or equal to about 1, wherein h is lamella thickness upon droplet impingement onto the surface.

12. The article of any one of the preceding claims, wherein the article is a wind turbine blade, the macro-scale features comprise ridges having height A_r and spacing λ_r, and wherein 0.0001 mm < A_r and $\lambda_r \geq$ 0.0001 mm.

13. The article of any one of the preceding claims, wherein the article is a rainproof product, the macro-scale features comprise ridges having height A_r and spacing λ_r, and wherein 0.0001 mm < A_r and $\lambda_r \geq$ 0.0001 mm.

14. The article of any one of the preceding claims, wherein the article is a steam turbine blade, the macro-scale features comprise ridges having height A_r and spacing λ_r, and wherein 0.00001 mm < A_r and λ_r > 0.0001 mm.

15. The article of any one of the preceding claims, wherein the article is an exterior aircraft part, the macro-scale features comprise ridges having height A_r and spacing λ_r, and wherein 0.00001 mm < A_r and λ_r > 0.0001 mm.

16. The article of any one of the preceding claims, wherein the article is a gas turbine blade, the macro-scale features comprise ridges having height A_r and spacing λ_r, and wherein 0.00001 mm < A_r and λ_r > 0.0001 mm.

17. The article of any one of claims 1-8, wherein the macro-scale features comprise protrusions having height A_p and whose centers are separated by a distance λ_p, with A_p/h > 0.01 and $\lambda_p/A_p \geq 2$, wherein h is lamella thickness upon droplet impingement onto the surface.

18. The article of any one of claims 1-8, wherein the macro-scale features comprise protrusions having height A_p and whose centers are separated by a distance λ_p, with 100 > A_p/h > 0.01 and $\lambda_p/A_p \geq 2$, wherein h is lamella thickness upon droplet impingement onto the surface.

19. The article of any one of claims 1-8, wherein the macro-scale features comprise protrusions having height A_p and whose centers are separated by a distance λ_p, with 10 > A_p/h > 0.1 and $\lambda_p/A_p \geq 2$, wherein h is lamella thickness upon droplet impingement onto the surface.

20. The article of any one of claims 1-8 and 17-19, wherein the macro-scale features are hemispherical protrusions.

21. The article of any one of claims 1-8 and 17-20, wherein the article is a wind turbine blade, the macro-scale features comprise protrusions having height A_p and whose centers are separated by a distance λ_p, and wherein 0.0001 mm < A_p and $\lambda_p \geq$ 0.0002 mm.

22. The article of any one of claims 1-8 and 17-21, wherein the article is a rainproof product, the macro-scale features comprise protrusions having height A_p and whose centers are separated by a distance λ_p, and wherein 0.0001 mm < A_p and $\lambda_p \geq$ 0.0002 mm.

23. The article of any one of claims 1-8 and 17-22, wherein the article is a steam turbine blade, the macro-scale features comprise protrusions having height A_p and whose centers are separated by a distance λ_p, and wherein 0.00001 mm < A_p and $\lambda_p \geq$ 0.00002 mm.

24. The article of any one of claims 1-8 and 17-23, wherein the article is an exterior aircraft part, the macro-scale features comprise protrusions having height A_p and whose centers are separated by a distance λ_p, and wherein 0.00001 mm < A_p and $\lambda_p \geq$ 0.00002 mm.

25. The article of any one of claims 1-8 and 17-24, wherein the article is a gas turbine blade, the macro-scale features comprise protrusions having height A_p and whose centers are separated by a distance λ_p, and wherein 0.00001 mm < A_p and $\lambda_p \geq$ 0.00002 mm.

26. The article of any one of claims 1-8, wherein the macro-scale features comprise a sinusoidal profile having amplitude A_c and period λ_c, with $A_c/h > 0.01$ and $\lambda_c/A_c \geq 2$, wherein h is lamella thickness upon droplet impingement onto the surface.

27. The article of any one of claims 1-8, wherein the macro-scale features comprise a sinusoidal profile having amplitude A_c and period λ_c, with $100 > A_c/h > 0.01$ and $500 \geq \lambda_c/A_c \geq 2$, wherein h is lamella thickness upon droplet impingement onto the surface.

28. The article of any one of claims 1-8, wherein the macro-scale features comprise a sinusoidal profile having amplitude A_c and period λ_c, with $50 > A_c/h > 0.1$ and $500 \geq \lambda_c/A_c \geq 2$, wherein h is lamella thickness upon droplet impingement onto the surface.

29. The article of any one of claims 1-8 and 26-28, wherein the article is a rainproof product, the macro-scale features comprise a sinusoidal profile having amplitude A_c and period λ_c, and wherein 0.0001 mm < A_c and $\lambda_c \geq$ 0.0002 mm.

30. The article of any one of claims 1-8 and 26-29, wherein the article is a wind turbine blade, the macro-scale features comprise a sinusoidal profile having amplitude A_c and period λ_c, and wherein 0.0001 mm < A_c and $\lambda_c \geq$ 0.0002 mm.

31. The article of any one of claims 1-8 and 26-30, wherein the article is a steam turbine blade, the macro-scale features comprise a sinusoidal profile having amplitude A_c and period λ_c, and wherein 0.00001 mm < A_c and $\lambda_c \geq$ 0.00002 mm.

32. The article of any one of claims 1-8 and 26-31, wherein the article is an exterior aircraft part, the macro-scale features comprise a sinusoidal profile having amplitude A_c and period λ_c, and wherein 0.00001 mm < A_c and $\lambda_c \geq$ 0.00002 mm.

33. The article of any one of claims 1-8 and 26-32, wherein the article is a gas turbine blade, the macro-scale features comprise a sinusoidal profile having amplitude A_c and period λ_c, and wherein 0.00001 mm < A_c and $\lambda_c \geq$ 0.00002 mm.

34. The article of any one of the preceding claims, wherein the surface comprises an alkane.

35. The article of any one of the preceding claims, wherein the surface comprises a fluoropolymer.

36. The article of any one of the preceding claims, wherein the surface comprises at least one member selected from the group consisting of teflon, trichloro(1H,1H,2H,2H-perfluorooctyl)silane (TCS), octadecyltrichlorosilane (OTS), heptadecafluoro- 1,1,2,2-tetrahydrodecyltrichlorosilane, fluoroPOSS, a ceramic material, a polymeric material, a fluorinated material, an intermetallic compound, and a composite material.

37. The article of any one of the preceding claims, wherein the surface comprises a polymeric material, the polymeric material comprising at least one of polytetrafluoroethylene, fluoroacrylate, fluoroeurathane, fluorosilicone, fluorosilane, modified carbonate, chlorosilanes, and silicone.

38. The article of any one of the preceding claims, wherein the surface comprises a ceramic material, the ceramic material comprising at least one of titanium carbide, titanium nitride, chromium nitride, boron nitride, chromium carbide, molybdenum carbide, titanium carbonitride, electroless nickel, zirconium nitride, fluorinated silicon dioxide, titanium dioxide, tantalum oxide, tantalum nitride, diamond-like carbon, and fluorinated diamond-like carbon.

39. The article of any one of the preceding claims, wherein the surface comprises an intermetallic compound, the intermetallic compound comprising at least one of nickel aluminide and titanium aluminide.

40. The article of any one of the preceding claims, wherein the article is a condenser.

41. The article of any one of the preceding claims, wherein the article is a drip shield for storage of radioactive material.

42. The article of any one of the preceding claims, wherein the article is a self-cleaning solar panel.

43. An atomizer comprising a non-wetting surface having a dynamic contact angle of at least about 90°, said surface patterned with macro-scale features configured to induce controlled asymmetry in a liquid film produced by impingement of a droplet onto the surface, thereby promoting breakup of the droplet on the surface.

44. The atomizer of claim 43, wherein the non-wetting surface is supermetallophobic.

45. The atomizer of claim 43, wherein the droplet comprises a molten metal.

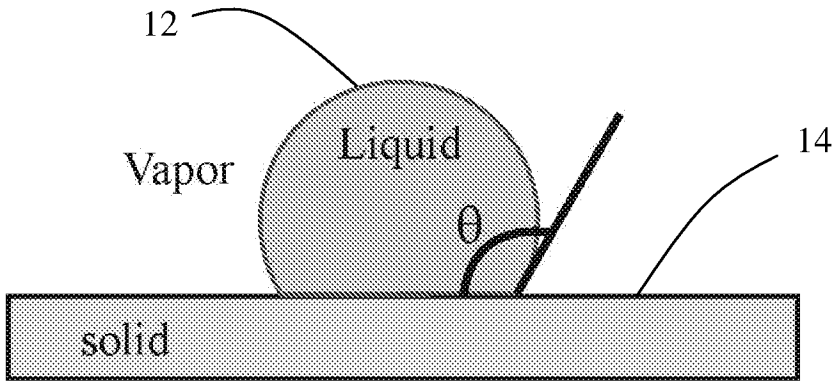

FIG. 1a

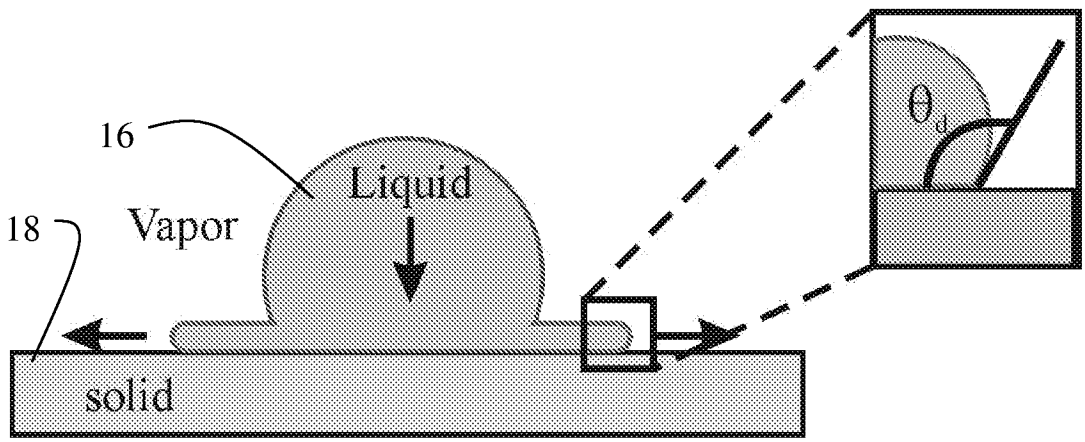

FIG. 1b

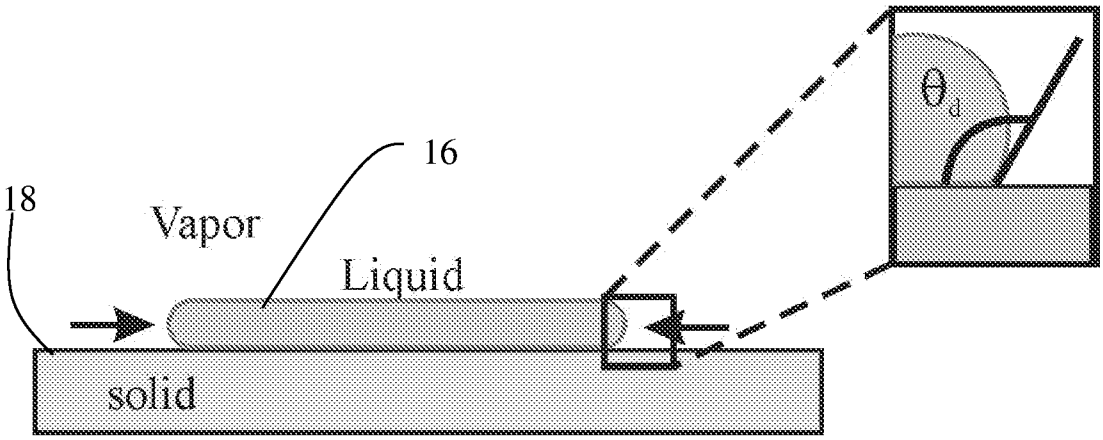

FIG. 1c

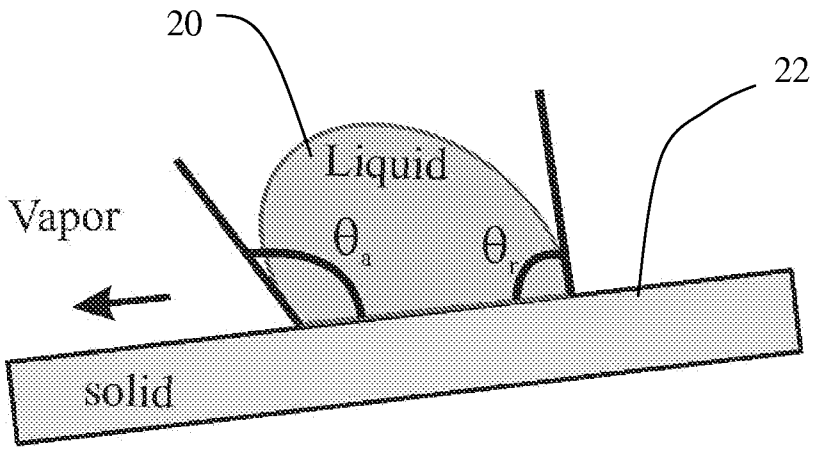

FIG. 1d

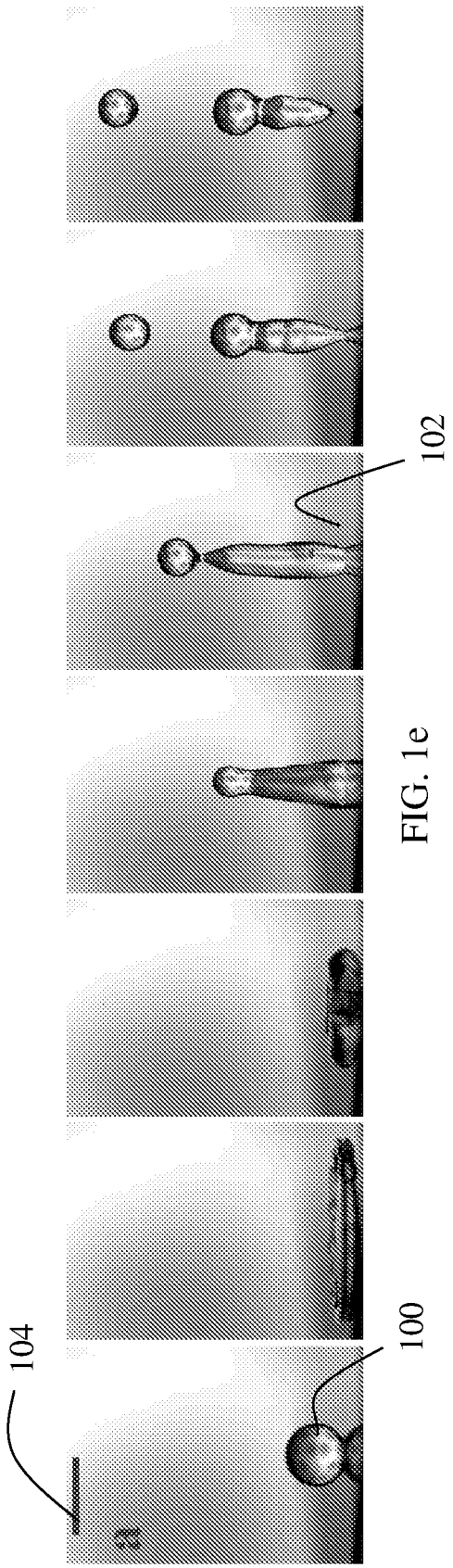

FIG. 1e

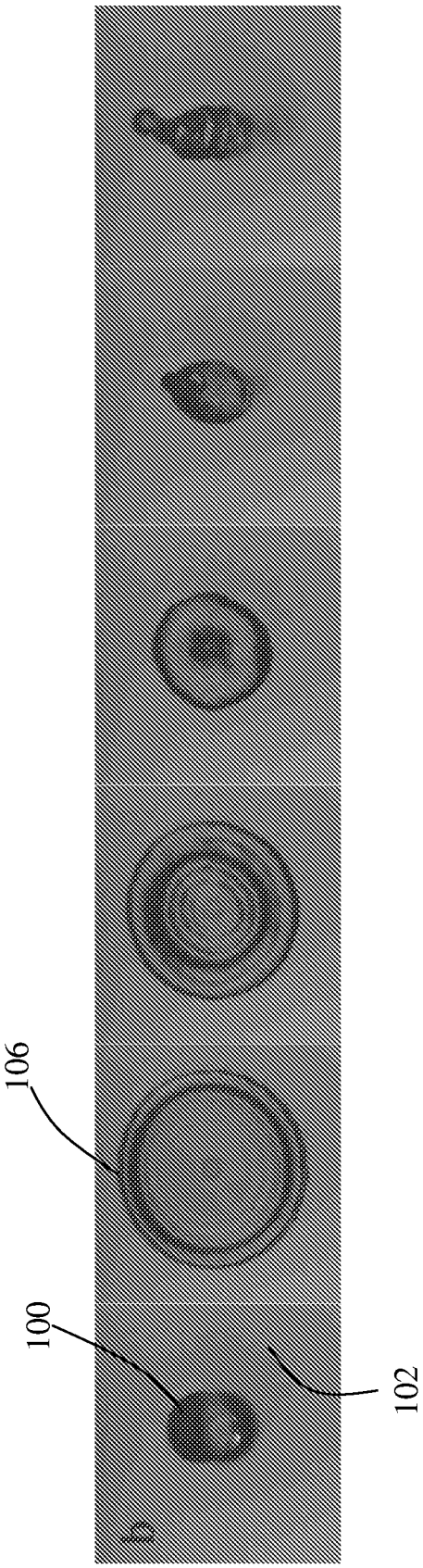

FIG. 1f

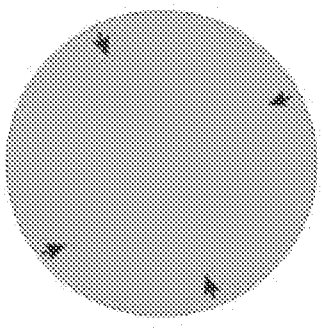

FIG. 2a

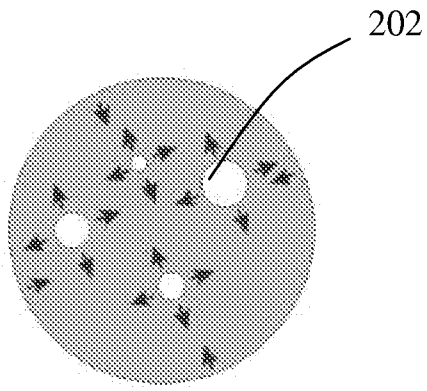

FIG. 2b

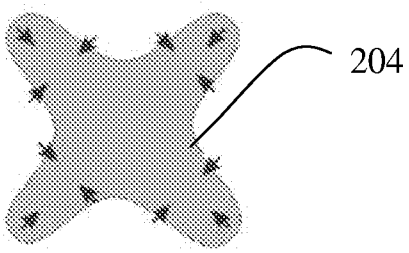

FIG. 2c

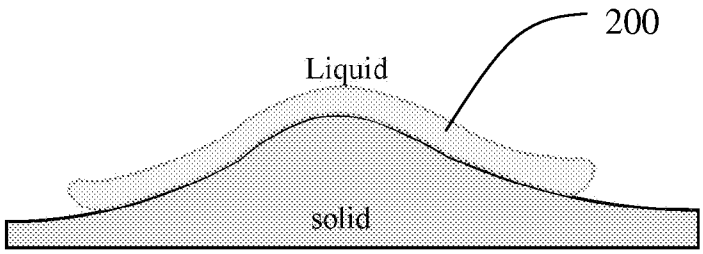

FIG. 2d

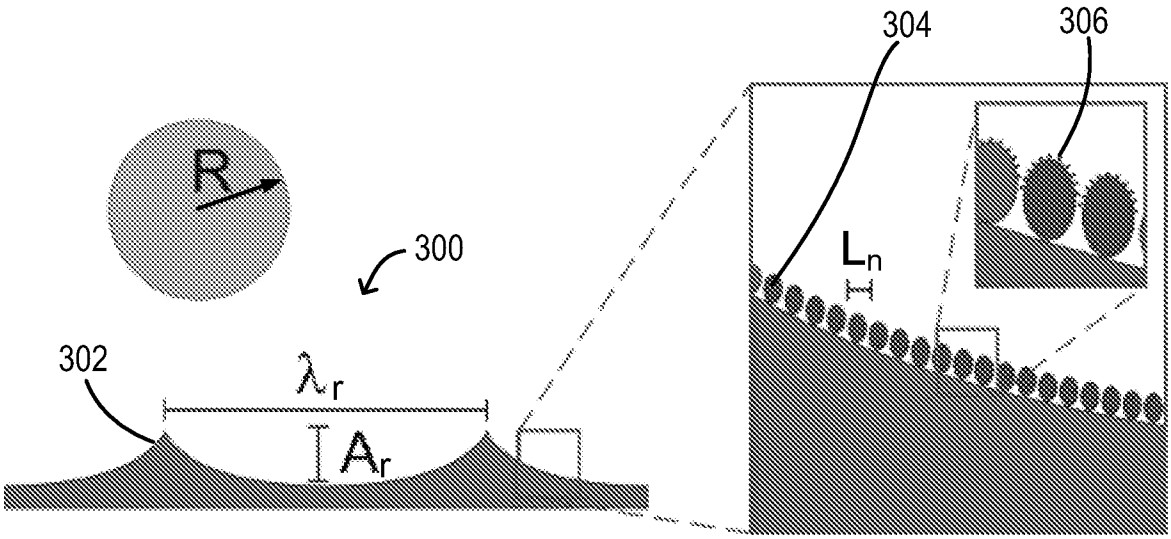

FIG. 3

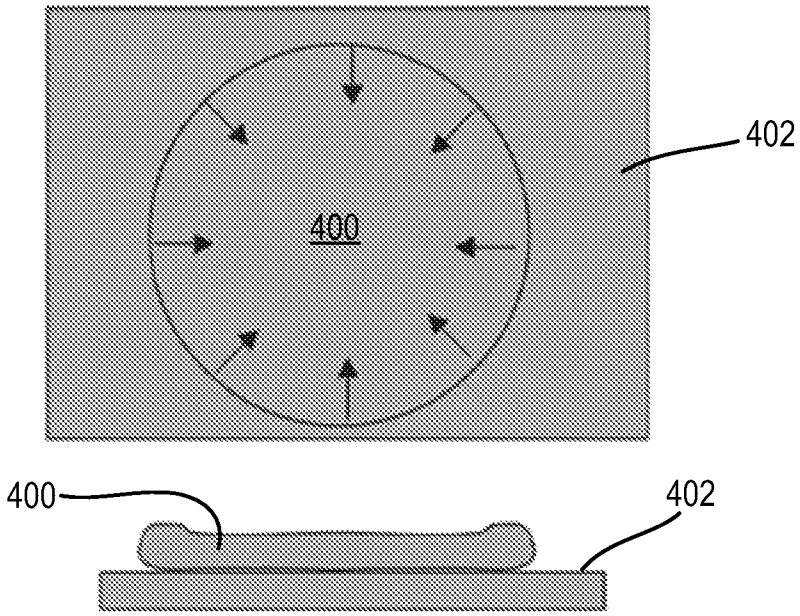

FIG. 4

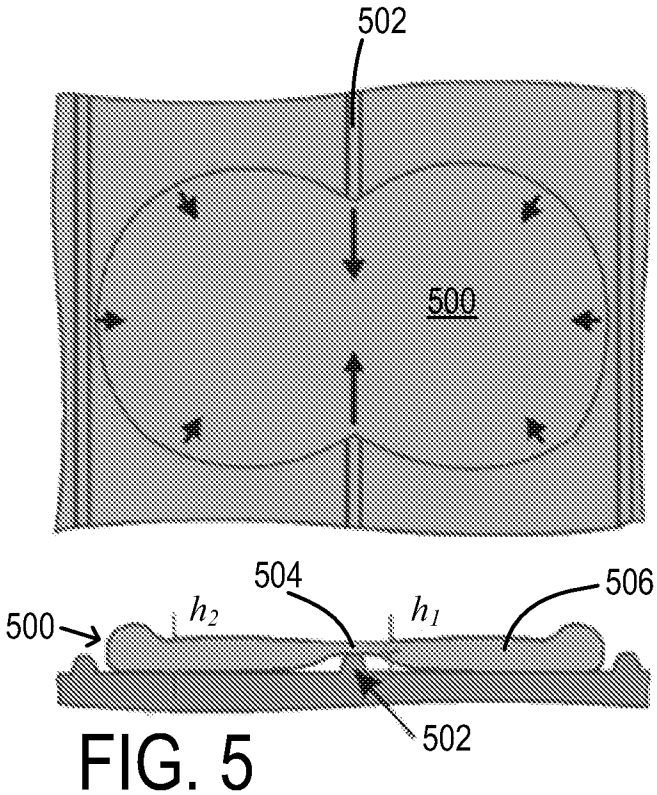

FIG. 5

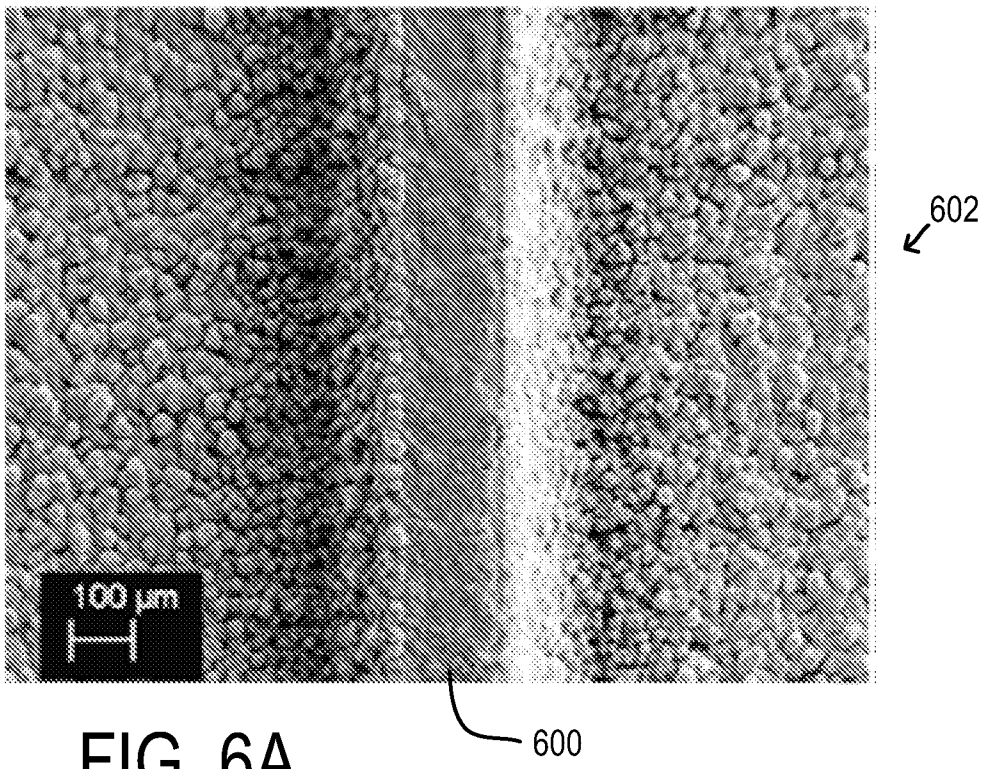

FIG. 6A

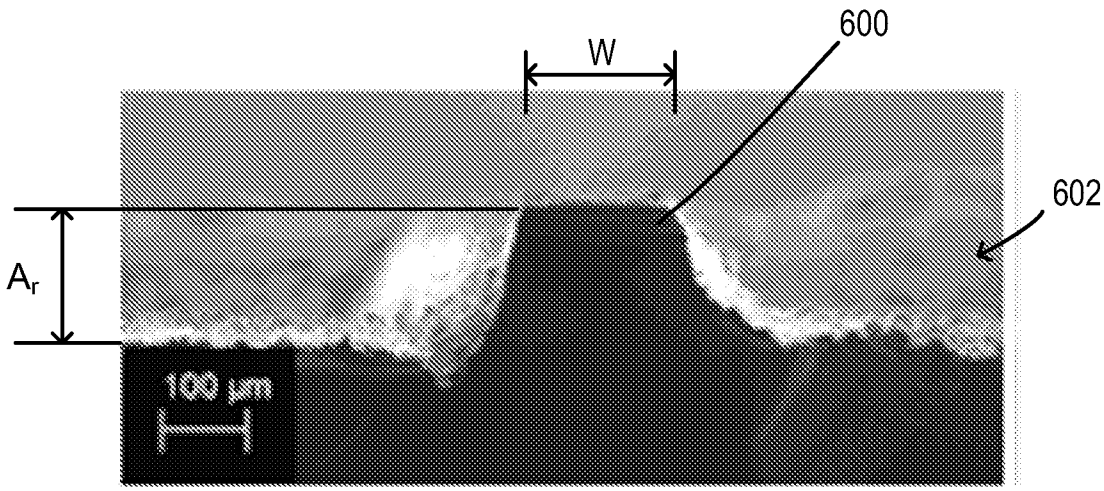

FIG. 6B

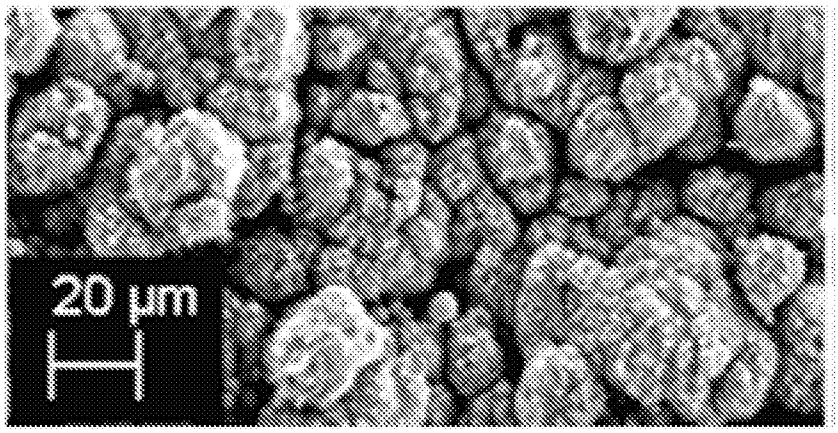

FIG. 6C

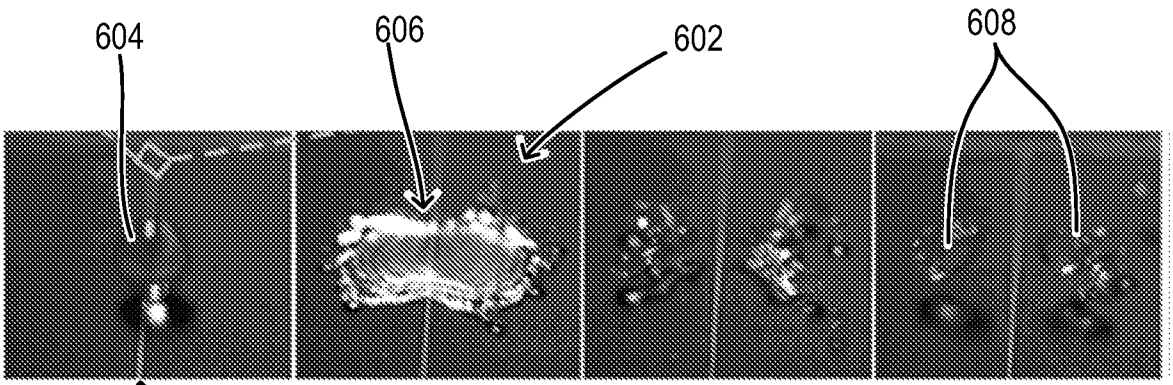

FIG. 6D

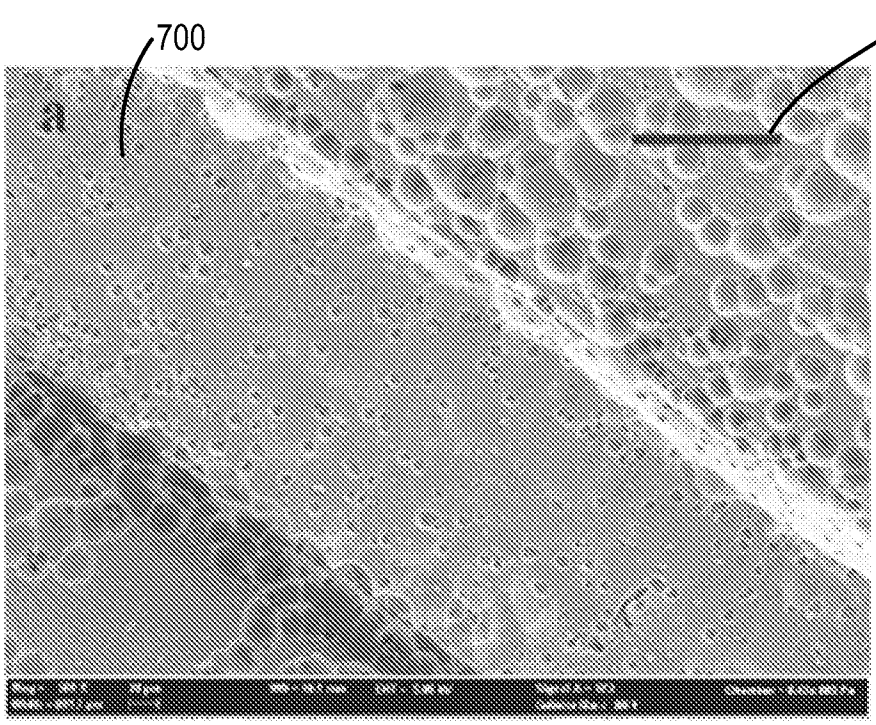

FIG. 7A

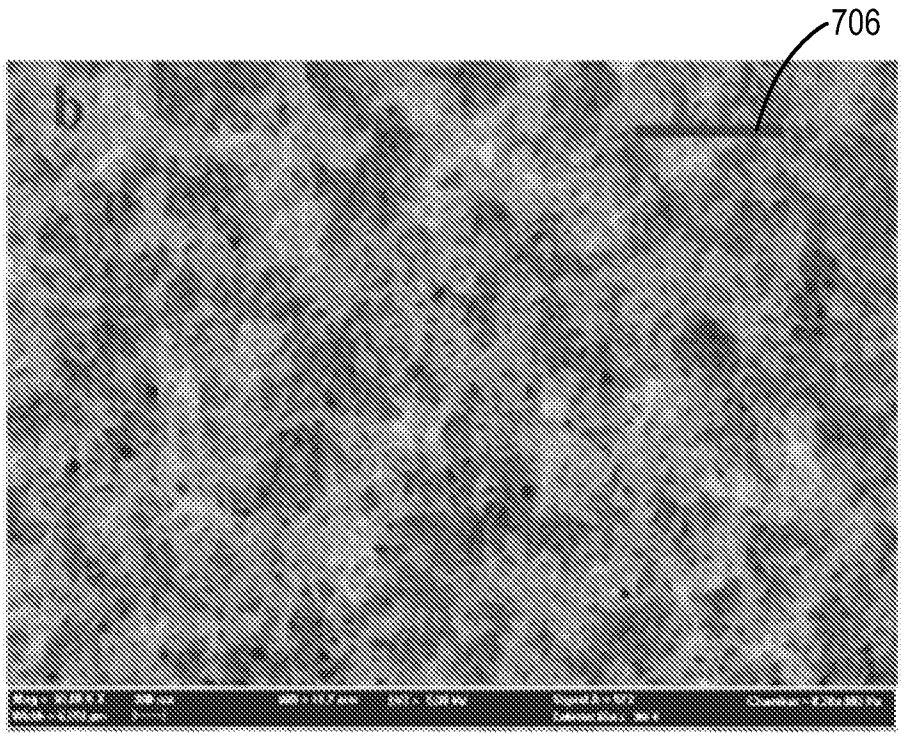

FIG. 7B

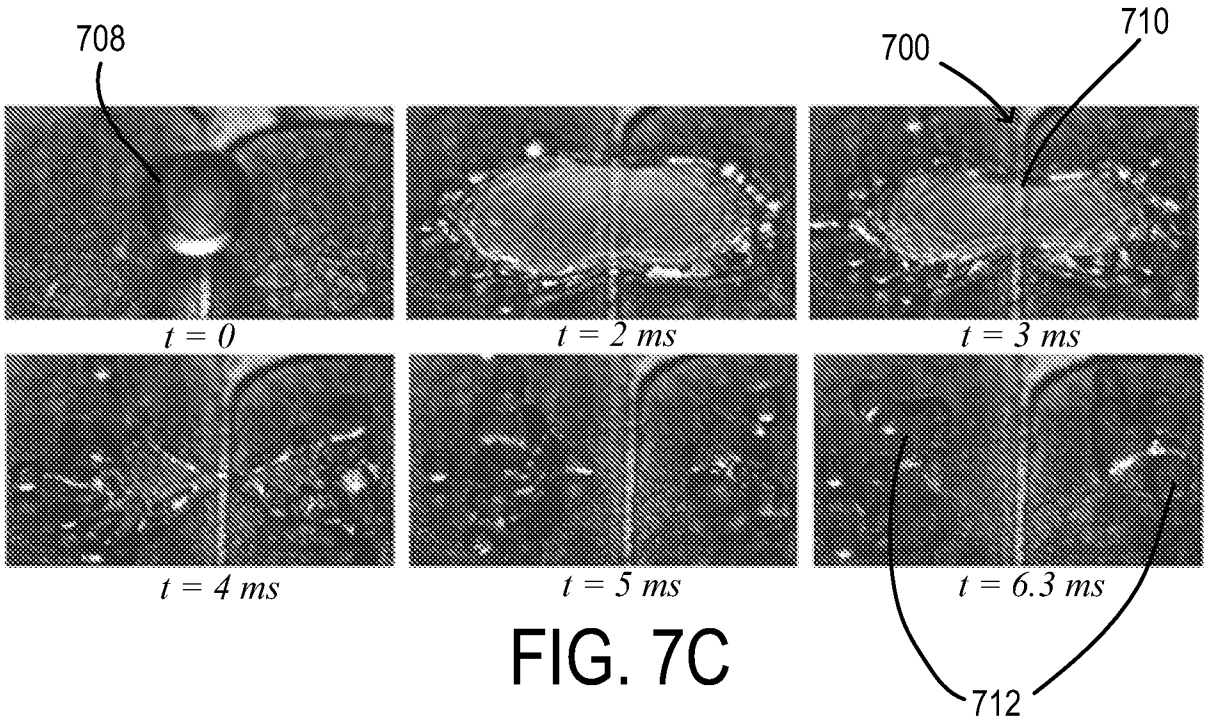

FIG. 7C

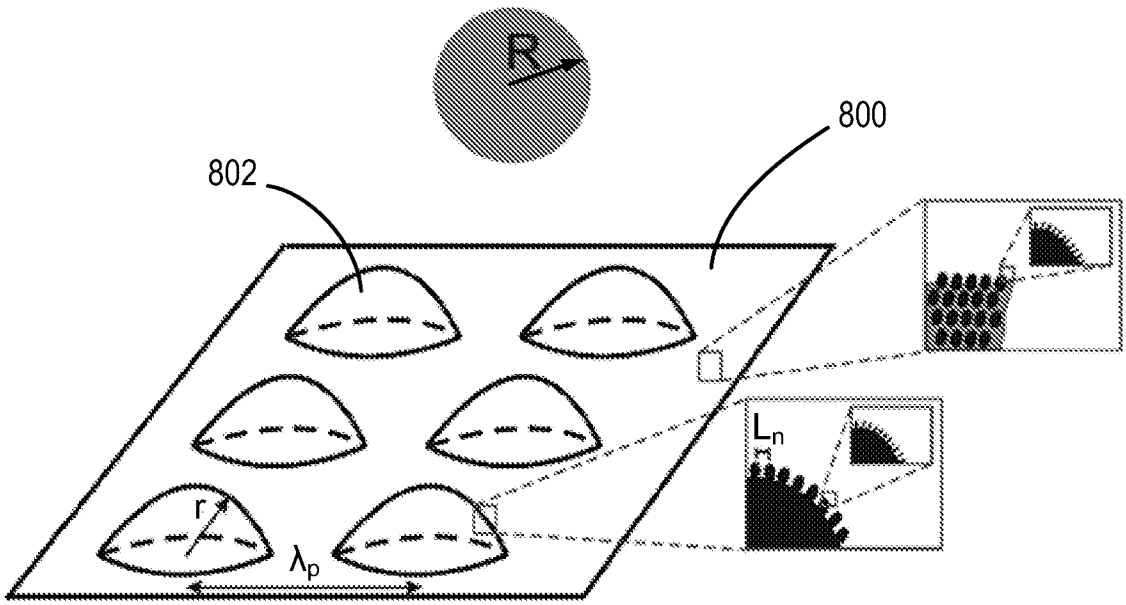

FIG. 8

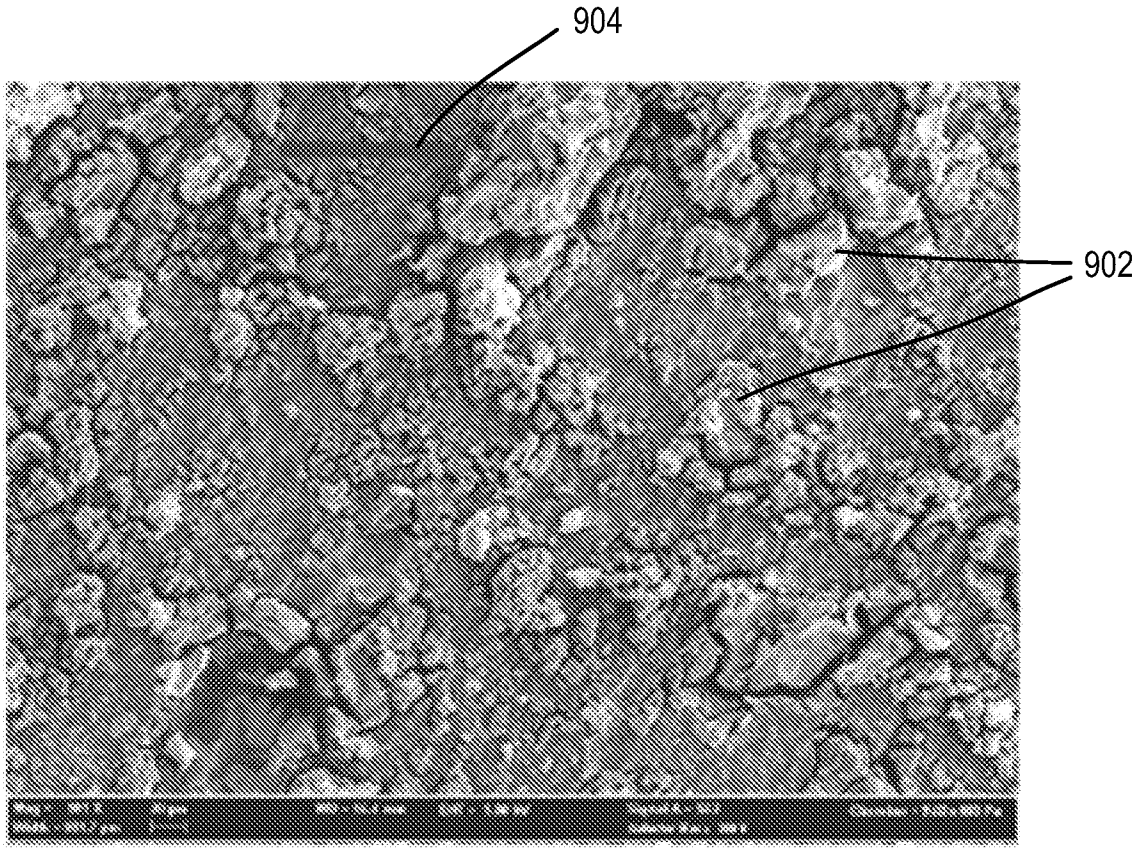

FIG. 9A

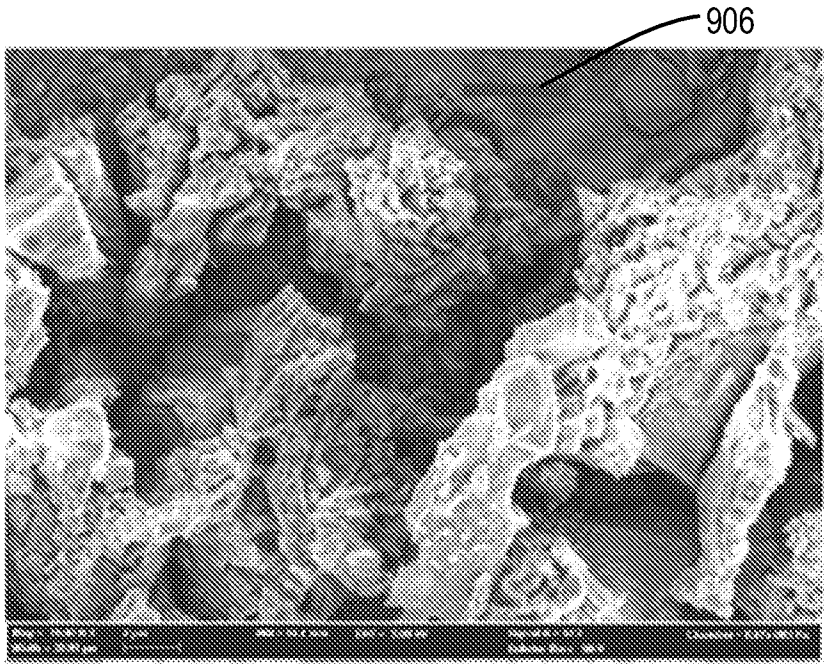

FIG. 9B

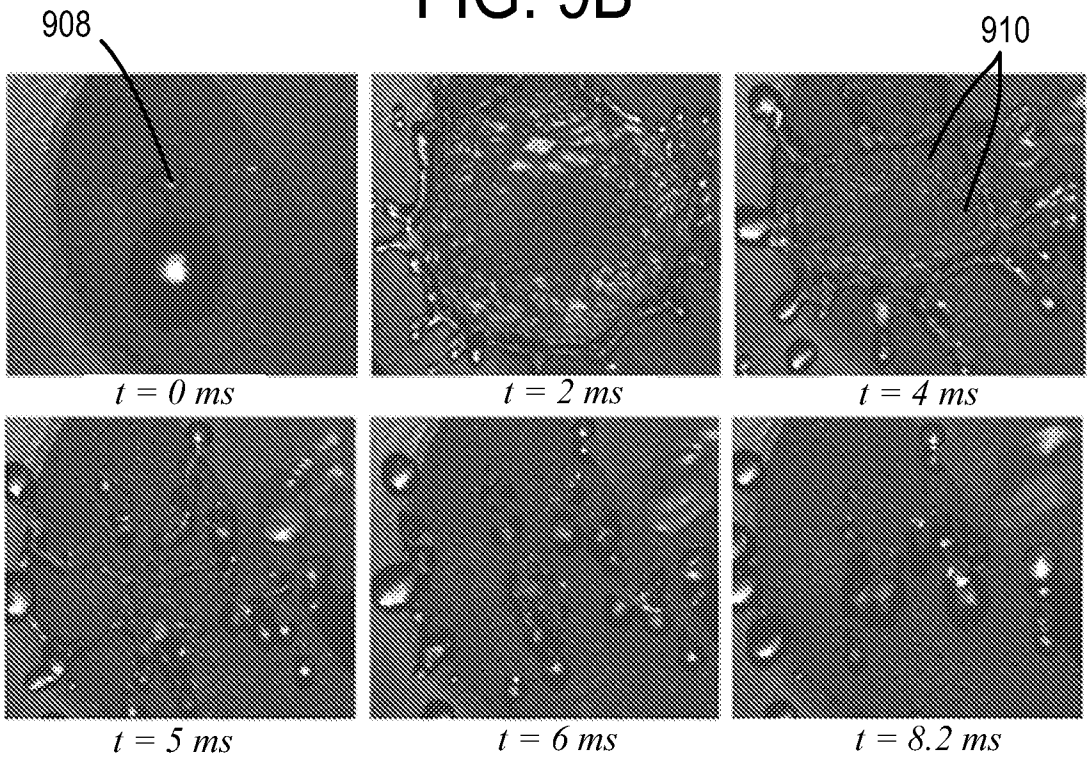

FIG. 9C

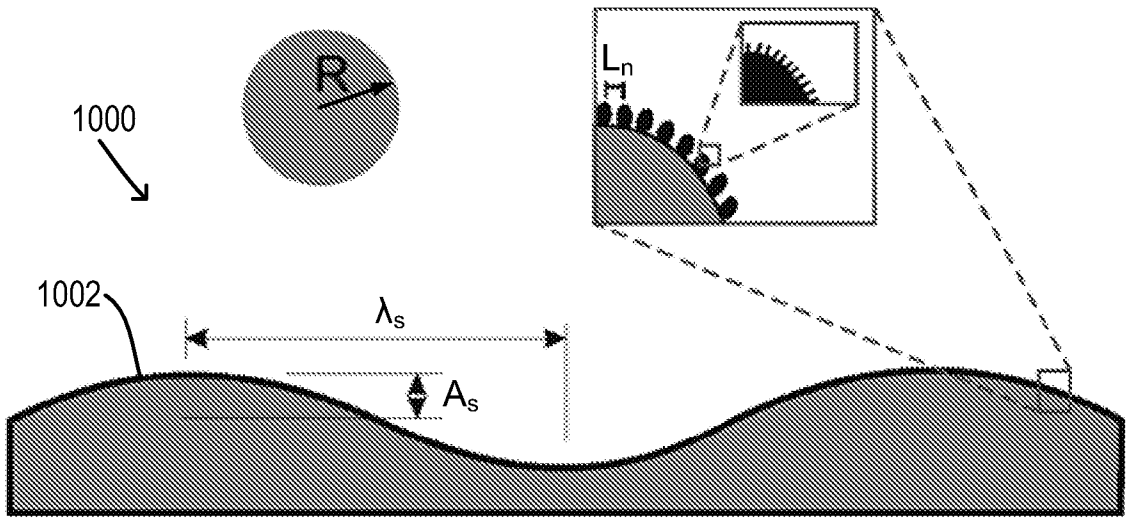

FIG. 10

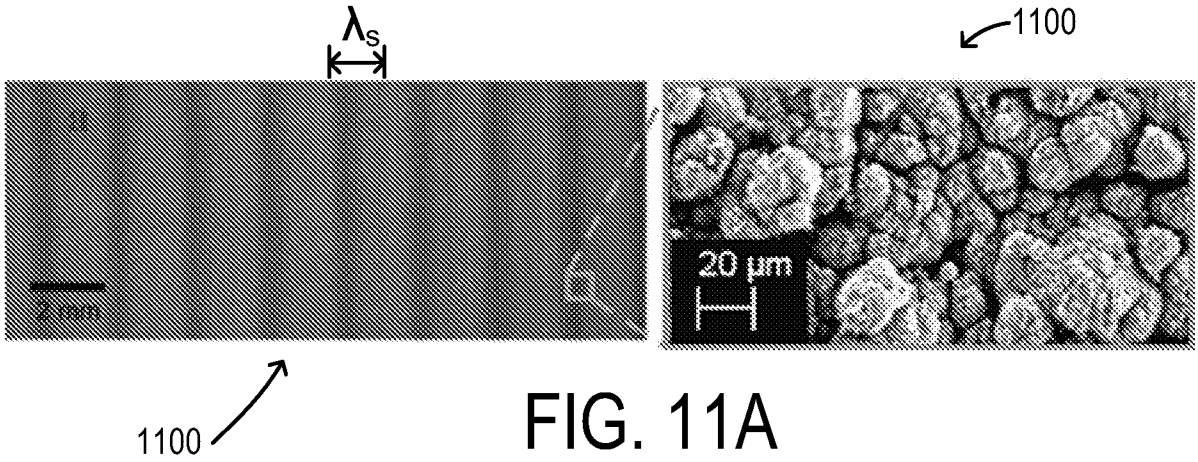

FIG. 11A

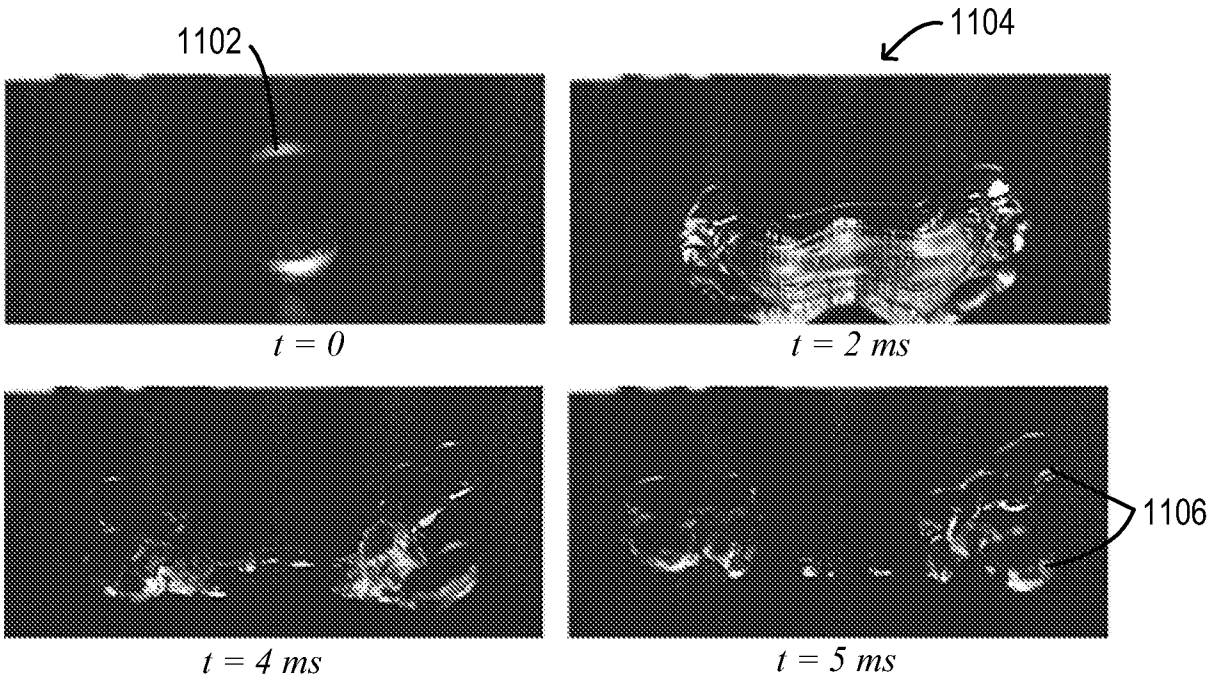

FIG. 11B

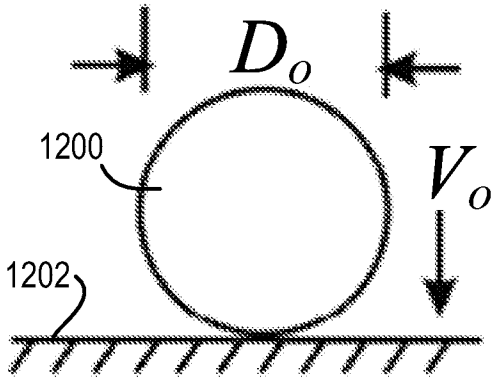

FIG. 12A

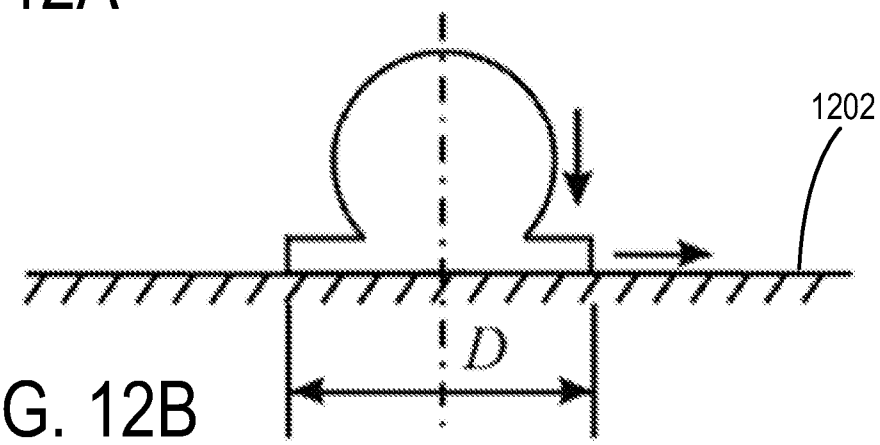

FIG. 12B

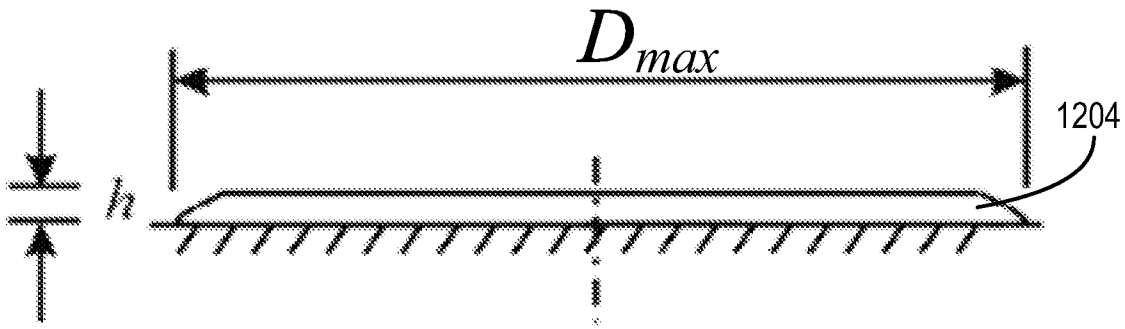

FIG. 12C

INTERNATIONAL SEARCH REPORT

International application No
PCT/US2011/061498

A. CLASSIFICATION OF SUBJECT MATTER
INV. B82Y30/00 B05D5/08 B08B17/06
ADD.

According to International Patent Classification (IPC) or to both national classification and IPC

B. FIELDS SEARCHED

Minimum documentation searched (classification system followed by classification symbols)
B82Y B05D B08B

Documentation searched other than minimum documentation to the extent that such documents are included in the fields searched

Electronic data base consulted during the international search (name of data base and, where practicable, search terms used)
EPO-Internal

C. DOCUMENTS CONSIDERED TO BE RELEVANT

Category*	Citation of document, with indication, where appropriate, of the relevant passages	Relevant to claim No.
X	POZZATO A ET AL: "Superhydrophobic surfaces fabricated by nanoimprint lithography", MICROELECTRONIC ENGINEERING, ELSEVIER PUBLISHERS BV., AMSTERDAM, NL, vol. 83, no. 4-9, 1 April 2006 (2006-04-01), pages 884-888, XP024954955, ISSN: 0167-9317, DOI: 10.1016/J.MEE.2006.01.012 [retrieved on 2006-04-01]	1,2,5,6, 9-13, 34-37
Y	pages 885-887; figures 1-5	7,14-33, 38-42

-/--

[X] Further documents are listed in the continuation of Box C. [ ] See patent family annex.

* Special categories of cited documents :

"A" document defining the general state of the art which is not considered to be of particular relevance

"E" earlier application or patent but published on or after the international filing date

"L" document which may throw doubts on priority claim(s) or which is cited to establish the publication date of another citation or other special reason (as specified)

"O" document referring to an oral disclosure, use, exhibition or other means

"P" document published prior to the international filing date but later than the priority date claimed

"T" later document published after the international filing date or priority date and not in conflict with the application but cited to understand the principle or theory underlying the invention

"X" document of particular relevance; the claimed invention cannot be considered novel or cannot be considered to involve an inventive step when the document is taken alone

"Y" document of particular relevance; the claimed invention cannot be considered to involve an inventive step when the document is combined with one or more other such documents, such combination being obvious to a person skilled in the art

"&" document member of the same patent family

Date of the actual completion of the international search	Date of mailing of the international search report
24 April 2012	31/07/2012

Name and mailing address of the ISA/	Authorized officer
European Patent Office, P.B. 5818 Patentlaan 2 NL - 2280 HV Rijswijk Tel. (+31-70) 340-2040, Fax: (+31-70) 340-3016	Michalitsch, Richard

3

Form PCT/ISA/210 (second sheet) (April 2005)

C(Continuation). DOCUMENTS CONSIDERED TO BE RELEVANT

Category*	Citation of document, with indication, where appropriate, of the relevant passages	Relevant to claim No.
X	XIYING LI ET AL: "Dynamic Behavior of the Water Droplet Impact on a Textured Hydrophobic/Superhydrophobic Surface: The Effect of the Remaining Liquid Film Arising on the Pillars' Tops on the Contact Time", LANGMUIR, vol. 26, no. 7, 6 April 2010 (2010-04-06), pages 4831-4838, XP055024383, ISSN: 0743-7463, DOI: 10.1021/la903603z	1,2,5,6, 9-13, 34-37
Y	the whole document	7,14-33, 38-42

X	DENG TAO ET AL: "Nonwetting of impinging droplets on textured surfaces", APPLIED PHYSICS LETTERS, AIP, AMERICAN INSTITUTE OF PHYSICS, MELVILLE, NY, US, vol. 94, no. 13, 2 April 2009 (2009-04-02) , pages 133109-133109, XP012120716, ISSN: 0003-6951, DOI: 10.1063/1.3110054	1,2,5,6, 9-13, 34-37
Y	the whole document	7,14-33, 38-42

X	VARANASI KRIPA ET AL: "Frost formation and ice adhesion on superhydrophobic surfaces", APPLIED PHYSICS LETTERS, AIP, AMERICAN INSTITUTE OF PHYSICS, MELVILLE, NY, US, vol. 97, no. 23, 7 December 2010 (2010-12-07), pages 234102-234102, XP012138070, ISSN: 0003-6951, DOI: 10.1063/1.3524513	1,2,5,6, 34-37
Y	the whole document	7,9-33, 38-42

X	JAE BONG LEE ET AL: "Dynamic Wetting and Spreading Characteristics of a Liquid Droplet Impinging on Hydrophobic Textured Surfaces", LANGMUIR, 1 January 2011 (2011-01-01), XP055024385, ISSN: 0743-7463, DOI: 10.1021/la104829x	1,2,5,6, 34-37
Y	page 6566 - page 6568; figures 1-4	7,9-33, 38-42

3

INTERNATIONAL SEARCH REPORT

International application No.
PCT/US2011/061498

Box No. II Observations where certain claims were found unsearchable (Continuation of item 2 of first sheet)

This international search report has not been established in respect of certain claims under Article 17(2)(a) for the following reasons:

1. ☐ Claims Nos.:
because they relate to subject matter not required to be searched by this Authority, namely:

2. ☐ Claims Nos.:
because they relate to parts of the international application that do not comply with the prescribed requirements to such an extent that no meaningful international search can be carried out, specifically:

3. ☐ Claims Nos.:
because they are dependent claims and are not drafted in accordance with the second and third sentences of Rule 6.4(a).

Box No. III Observations where unity of invention is lacking (Continuation of item 3 of first sheet)

This International Searching Authority found multiple inventions in this international application, as follows:

see additional sheet

1. ☐ As all required additional search fees were timely paid by the applicant, this international search report covers all searchable claims.

2. ☐ As all searchable claims could be searched without effort justifying an additional fees, this Authority did not invite payment of additional fees.

3. ☐ As only some of the required additional search fees were timely paid by the applicant, this international search report covers only those claims for which fees were paid, specifically claims Nos.:

4. ☒ No required additional search fees were timely paid by the applicant. Consequently, this international search report is restricted to the invention first mentioned in the claims; it is covered by claims Nos.:

1, 2(completely); 5-42(partially)

Remark on Protest

☐ The additional search fees were accompanied by the applicant's protest and, where applicable, the payment of a protest fee.

☐ The additional search fees were accompanied by the applicant's protest but the applicable protest fee was not paid within the time limit specified in the invitation.

☐ No protest accompanied the payment of additional search fees.

FURTHER INFORMATION CONTINUED FROM PCT/ISA/ 210

This International Searching Authority found multiple (groups of) inventions in this international application, as follows:

1. claims: 1, 2(completely); 5-42(partially)

   An article comprising a non-wetting surface having a dynamic contact angle of at least about 90°, wherein the surface is superhydrophobic and patterned with macro-scale features.

   ---

2. claims: 1, 3(completely); 5-42(partially)

   An article comprising a non-wetting surface having a dynamic contact angle of at least about 90°, wherein the surface is superoleophobic and patterned with macro-scale features.

   ---

3. claims: 1, 4, 43-45(completely); 5-42(partially)

   An article comprising a non-wetting surface having a dynamic contact angle of at least about 90°, wherein the surface is supermetallophobic and patterned with macro-scale features.
